

Copyright Warning & Restrictions

The copyright law of the United States (Title 17, United States Code) governs the making of photocopies or other reproductions of copyrighted material.

Under certain conditions specified in the law, libraries and archives are authorized to furnish a photocopy or other reproduction. One of these specified conditions is that the photocopy or reproduction is not to be “used for any purpose other than private study, scholarship, or research.” If a user makes a request for, or later uses, a photocopy or reproduction for purposes in excess of “fair use” that user may be liable for copyright infringement,

This institution reserves the right to refuse to accept a copying order if, in its judgment, fulfillment of the order would involve violation of copyright law.

Please Note: The author retains the copyright while the New Jersey Institute of Technology reserves the right to distribute this thesis or dissertation

Printing note: If you do not wish to print this page, then select “Pages from: first page # to: last page #” on the print dialog screen

The Van Houten library has removed some of the personal information and all signatures from the approval page and biographical sketches of theses and dissertations in order to protect the identity of NJIT graduates and faculty.

ABSTRACT

DECIPHERING THE BIOLOGY OF AXON STRETCH-GROWTH

by

Joseph R. Loverde

Traditional nerve regeneration strategies focus on growth cone-mediated growth, a form of nerve growth that occurs primarily during embryogenesis. Early axons continue to grow from the end distal to the soma, seeking targets on which to synapse. It is believed that once the axons synapse, stretch-growth takes over and is responsible for the great lengths achieved by nerves of the central and peripheral nervous systems. Recent work has demonstrated stretch-growth *in vitro* resulting in dramatically increased growth rates compared to the growth cone. Here, the aim was to decipher the underlying biology associated with axon stretch-growth using two approaches. First, a device was created for live imaging of stretch-growth as it occurs on the stage of a microscope. Morphology changes and cytoskeletal transport were captured live at up to 600x magnification over six days of culturing. Second, the RNA species produced during stretch-growth were isolated in order to reveal the regulatory genes involved in this process. Successive RNA quantifications have revealed up to a three-fold increase in RNA population of stretch-grown tissue when compared to controls.

DECIPHERING THE BIOLOGY OF AXON STRETCH-GROWTH

by
Joseph R. Loverde

**A Thesis
Submitted to the Faculty of
New Jersey Institute of Technology
in Partial Fulfillment of the Requirements for the Degree of
Master of Science in Biomedical Engineering**

Department of Biomedical Engineering

January 2009

Blank Page

APPROVAL PAGE

DECIPHERING THE BIOLOGY OF AXON STRETCH-GROWTH

Joseph R. Loverde

12/9/08

Dr. Bryan J. Pfister, Thesis Advisor
Assistant Professor of Biomedical Engineering, NJIT

Date

12/9/08

Dr. Patricia Soteropoulos, Committee Member
Director, Center for Applied Genomics
Assistant Professor, Public Health Research Institute
UMDNJ-New Jersey Medical School

Date

12/9/08

Dr. Cheul H. Cho, Committee Member
Assistant Professor of Biomedical Engineering, NJIT

Date

BIOGRAPHICAL SKETCH

Author: Joseph R. Loverde

Degree: Master of Science

Date: January 2009

Undergraduate and Graduate Education:

- Master of Science in Biomedical Engineering,
New Jersey Institute of Technology, Newark, NJ, 2009
- Master of Science in Bioinformatics,
Northeastern University, Boston, MA, 2005
- Bachelor of Science in Biology,
Muhlenberg College, Allentown, PA, 1999

Major: Biomedical Engineering

Presentations and Publications:

Loverde J. R., Ozoka V.C., Miller K.E., Pfister B.J.

“Live Imaging of Extreme Axon Stretch-Growth,” Society for Neuroscience 38th
Annual Meeting, Washington, D.C., November 2008.

Kiessling A. A., Desmarais B.M., Yin H.Z., Loverde J., Eyre R.C. (2008). Detection and
Identification of Bacterial DNA in Semen. *Fertility and Sterility*, 90, 1744-1756.

I would like to dedicate this work to my father, Joseph A. Lo Verde, for his relentless support of my endeavors. Through him, I have learned not to fear arduous challenge, but to scrutinize details and succeed by design. It is with his rigor that I aspire to continue in research.

ACKNOWLEDGMENT

I would like to thank the many people who have helped make this work possible. I would like to thank Dr. Bryan Pfister, my mentor, for continuing to inspire me to explore new and fascinating research. Dr. Patricia Soteropoulos spent considerable time with me in consultation on the design of gene array experiments. I would like to thank Dr. Cheul Cho for his participation in review of this thesis. Vivian Ozoka and Rob Aquino spent significant time designing the live imaging bioreactor together with the help of their Capstone Design Team. I would also like to thank John Hoinowski for his time, advice, and work in designing and building the bioreactor.

TABLE OF CONTENTS

Chapter	Page
1 INTRODUCTION	1
1.1 Background Information	1
1.2 Objectives	3
2 DESIGN OF LIVE IMAGING STRETCH-GROWTH BIOREACTOR	5
2.1 Culture Chamber	5
2.2 Viewing Window	6
2.3 Stretch-Growth	7
2.3.1 Culture Chamber Interior	7
2.3.2 Culture Chamber Exterior	9
2.4 Gas and Humidity	11
2.5 Temperature	12
2.6 Mounting and Plumbing	12
3 DESIGN OF STRETCH-GROWTH GENE EXPRESSION EXPERIMENT	15
4 RESULTS	18
4.1 Live Imaging Stretch-Growth Bioreactor	18
4.1.1 Experimental Protocol	18
4.1.2 Culture Chamber	20
4.1.3 Viewing Window	20
4.1.4 Temperature	20
4.1.5 Gas and Humidity	21

TABLE OF CONTENTS
(Continued)

Chapter	Page
4.1.6 Stretch-Growth	22
4.1.7 Mounting and Plumbing	22
4.1.8 Bright Field Live Imaging	23
4.1.9 Fluorescence Live Imaging	26
4.2 Stretch-Growth Gene Expression	28
4.2.1 Growth of Tissue and Isolation of RNA	28
4.2.2 Quantification and Visualization of RNA	33
4.2.3 Microarray Analysis	35
5 DISCUSSION	36
5.1 Live Imaging Stretch-Growth Bioreactor	36
5.2 Stretch-Growth Gene Expression	37
APPENDIX A DORSAL ROOT GANGLIA ISOLATION	39
APPENDIX B DORSAL ROOT GANGLIA PLATING	40
APPENDIX C DORSAL ROOT GANGLIA CULTURE	41
APPENDIX D STRETCH-GROWTH SPECIFICATIONS	42
APPENDIX E RNA ISOLATION PROTOCOL	43
APPENDIX F RNA GEL ELECTROPHORESIS	45
REFERENCES	48

LIST OF TABLES

Table		Page
4.1	RNA Quantification	34
D.1	Step Motor and Table Specifications	42
D.2	Stretch-growth Schedule	42

LIST OF FIGURES

Figure	Page
2.1 Culture chamber	6
2.2 Culture chamber lid. Flush mounted ports prevent interference with towing block and culture while promoting uniform flow of gas	6
2.3 Cover glass viewing window	7
2.4 University of Pennsylvania extreme stretch-growth frame illustrating a single lane of stretch-grown axons. (A) Starting position of towing block. (B) Stretch-grown axons visible. (C) Stretch-growth completed as towing block reaches limit of travel	8
2.5 Live imaging stretch-growth bioreactor culture chamber. Three lanes visible, translucent Aclar strips attached to towing block and making contact with cover glass	8
2.6 Exterior culture chamber stretch-growth components. Linear-motion table located behind the culture chamber interfaces with towing rods via ABS brace. External screws of braking mechanism shown disengaged	10
2.7 Screen-shot of SI Programmer controller software used for stretch-growth	10
2.8 Erlenmeyer flask within heated water-bath. Gas is bubbled through sterile water for humidification prior to filtration and perfusion into culture chamber	11
2.9 Live imaging stretch-growth bioreactor atop delrin chassis, affixed to inverted microscope stage	13
2.10 Complete live imaging stretch-growth system	14
3.1 Stretch-growth bioreactors developed at the University of Pennsylvania	16
4.1 Temperature controller overrun upon initial heating from room temperature. Temperature was read from thermistor located within culture chamber lid above plated cells	21

LIST OF FIGURES
(Continued)

Figure	Page
4.2 Stretch-grown axons shown utilizing 4x objective. Bar = 500 μ m	23
4.3 Stretch-grown axons shown utilizing 10x objective. Bar = 100 μ m	24
4.4 Stretch-grown axons shown utilizing 10x objective. Bar = 100 μ m	24
4.5 Stretch-grown axons shown utilizing 60x objective. Bar = 50 μ m	25
4.6 Stretch-grown axon live imaging time-lapse shown utilizing 4x objective. Montage represents 14 hours of stretching with 1.5 hours between frames as recorded by Voodoo time-lapse software. Stretch rate of 2mm/day recorded over 1.2mm of stretch-growth. Aclar towing substrate can be seen moving outside field of view toward right edge	26
4.7 Stretch-grown axons stained for mitochondria, confocal microscopy shown utilizing 60x objective. Bar = 50 μ m	27
4.8 15 μ m Z-Stack volume render of stretch-grown axons stained for mitochondria, confocal microscopy shown utilizing 60x objective. Bar = 50 μ m	28
4.9 Aclar coating failure. Upper left corner shows peeling of stretch-grown axons away from the Aclar originally used in stretch-growth. Bar = 500 μ m	30
4.10 Stretch-grown axons. Aclar towing substrate visible along right edge. Bar = 500 μ m	30
4.11 Non-stretch-grown controls. Bar = 500 μ m	33
4.12 Gel electrophoresis of RNA stained with ethidium bromide and visualized by UV light, samples run top to bottom. (A&F) Invitrogen 0.24-9.5 Kb RNA ladder. (B&E) Non-stretch-grown control tissue. (C) 10mm/day stretch-grown tissue soma. (D) 10mm/day stretch-grown tissue axon	35

CHAPTER 1

INTRODUCTION

1.1 Background Information

Diseases and disorders of the Central Nervous System (CNS) affect approximately 50 million Americans. Conditions vary and include memory loss, addiction, schizophrenia, learning disabilities, depression, stroke, dementia, injury and others. Spinal Cord Injury (SCI) is one of the most debilitating, with an estimated 255,000 people currently living with SCI in the United States and 12,000 new cases per year. The estimated individual cost for SCI ranges from \$225,000 to \$775,000 for the first year, and an additional \$16,000 to \$140,000 annually depending on the severity of the injury. Total costs of CNS disorders are estimated to exceed \$400 billion per year in the United States [1, 15].

Significant nervous system research focuses on the growth of new nervous tissue. The majority of this research is based on growth cone mediated growth, the form of nerve growth that primarily occurs during embryogenesis and regeneration [3, 7, 8]. In a developing embryo, axons navigate via a growth cone over seemingly large distances to synapse with their targets. However, well after axons integrate and establish synaptic connections, animals and their nerves undergo a different and more significant form of growth. This second phase of growth is what drives the extension of short embryonic nerves into long adult nerves up to a meter long [2, 4, 12].

Research into both forms of growth has shown that axons require tension in order to prevent degeneration (shrinking of the axon). The extending growth cone provides the necessary tension in embryonic nerves. During the second phase of growth, coined

“stretch-growth,” tension is applied by the continuing growth of surrounding tissues. *In vitro* experiments have simulated stretch-growth by applying mechanical tension to axons grown from embryonic Dorsal Root Ganglia (DRG) neurons [2, 12]. Axons were allowed to synapse to a motile towing substrate, which was then drawn further away from the DRG soma in a continuous motion and sustained for a day or longer. More recent research has shown that stretch-growth can be exploited by the application of exponentially increasing stretch rate. A 10-fold increase in growth rate has been realized by *in vitro* stretch-growth utilizing a micro-stepper system when compared to growth cone growth [12].

Currently there is limited understanding of the fundamental biology of axon stretch-growth. The growth rates achievable by stretch-growth have created a paradox unexplainable by growth cone knowledge. Slow transport of the cytoskeletal proteins tubulin and neurofilament (the major cytoskeletal components of the axon) peaks at roughly 1 millimeter per day into the growth cone, the same limit found for growth cone extension. It was hypothesized that during stretch-growth this limit is exceeded as the rate of growth approaches 10 millimeters per day. Indeed, Bray has shown that the process can be inhibited by blockage of microtubule assembly, suggesting that transport of organelles and ribonucleic acid or protein must exceed the rates observed during growth cone growth [2].

Characterization of stretch-grown axons has been limited to static visualization of neurofilament, beta-tubulin, and tau protein. Transmission electron microscopy has revealed a 35% increase in the average cross-sectional area of stretch-grown axons, suggesting that axons increase in caliber as well as length resulting in a total volumetric

increase. In coordination with rapid axon growth, the number of sodium channels increased in stretch-grown axons, while both sodium and potassium channels increased in their respective soma [12].

1.2 Objectives

Here, two objectives were pursued in order to further develop our understanding of the stretch-growth process. The first was to develop a live imaging system capable of capturing the events that occur during stretch-growth. Such events include morphology changes, transport of organelles, and transport of RNA and protein species from the soma into the axon; all utilizing fluorescent markers. It was hypothesized that the governing cellular processes would be revealed, which could be exploited in future research.

The *in vitro* live imaging stretch-growth bioreactor must operate on the stage of a microscope, while simultaneously meeting the needs of physiological culture conditions. The stretch-growth bioreactor developed by Pfister et al. at the University of Pennsylvania was re-engineered in order to create a miniaturized version for live microscopic monitoring of the stretch-growth process. The central feature of this new system is a thin cover glass bottom that accommodates the working distance and optical properties required by high-magnification oil immersion objectives. The bioreactor itself now serves as an incubator, maintaining physiological temperature and pH while imaging experiments are performed over hours to days. Temperature is controlled by a closed loop system utilizing a thermistor and heating element. pH buffering of culture media is maintained by continuous perfusion of premixed 5% carbon dioxide, 95% oxygen gas.

Perfused gas is pre-warmed and humidified in order to minimize temperature fluctuation and evaporation of media.

The second objective was to develop a procedure to reveal the regulatory genes involved in axon stretch-growth. The design of gene expression experiments was done with the guidance of Dr. Patricia Soteropoulos from the Center for Applied Genomics at Public Health Research Institute (PHRI), UMDNJ-New Jersey Medical School. It was hypothesized that during stretch-growth, genes associated with the process are upregulated. Using bioreactors developed by Pfister et al. to generate sufficient quantity of stretch-grown tissue, a customized protocol was developed to isolate RNA from stretch-grown nervous tissue. The isolated RNA was quantified and run on a gel to determine quality prior to identification of active genes on an Affymetrix (Santa Clara, CA) DNA microarray. Non-stretch-grown controls (DRG neurons grown on tissue culture vessels under normal culture conditions without manipulations) were grown simultaneously alongside stretch-grown tissue for differential comparison of genes.

Both strategies were performed utilizing primary DRG neurons isolated from embryonic day 15 rat pups. Adult rats were mated 15 days prior to the scheduled isolation by Rutgers' Research Animal Facility (Newark, NJ). Pregnant rats were euthanized according to approved protocols and rat pups were removed by C-section.

There is currently a patent for Mechanically Elongated Neuronal Cells; patent number US 6,264,944 B1 which was invented by Douglas H. Smith from the University of Pennsylvania.

CHAPTER 2

DESIGN OF LIVE IMAGING STRETCH-GROWTH BIOREACTOR

The following chapter discusses the designs of the sub-systems that make up the live imaging stretch-growth bioreactor. The function of the newly redesigned sub-systems, as well as the specifications and choice of materials will be discussed for each sub-system. Lastly, the methods of assembly and sterilization will be noted.

2.1 Culture Chamber

The culture chamber (Figure 2.1) consists of a PolyEtherEtherKetone (PEEK) frame measuring 4.875" long by 3" wide by 1.5" tall. The lid consists of translucent 0.25" polycarbonate (Figure 2.2), facilitating observation of the culture and passage of light for microscopy. 316 Stainless Steel hardware and silicone gaskets fasten all components of the frame. These materials have repeatedly been shown to be biocompatible and corrosion resistant, while easily autoclaved for sterilization.

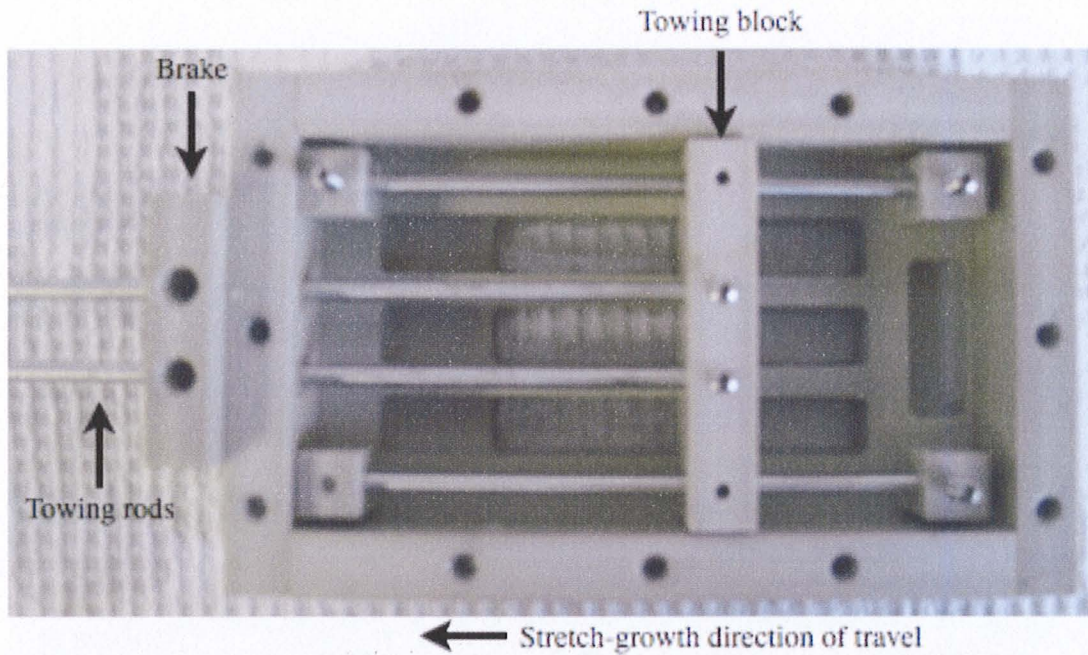


Figure 2.1 Culture chamber.

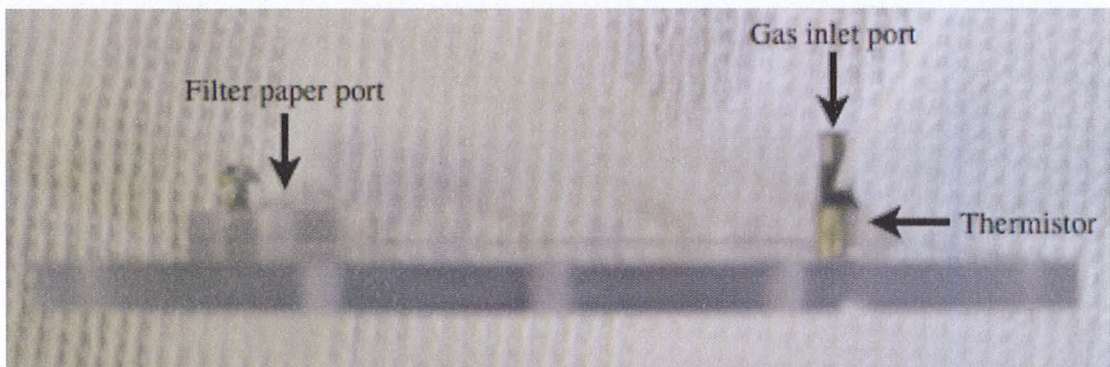


Figure 2.2 Culture chamber lid. Flush mounted ports prevent interference with towing block and culture while promoting uniform flow of gas.

2.2 Viewing Window

The bottom of the culture chamber is specially designed for high magnification viewing of stretch-grown axons on inverted microscopes. A 65mm long by 48mm wide by 0.16mm thick cover glass from Brain Research Laboratories (Newton, MA) serves as the

substrate for cell culture and as the bottom of the culture chamber. Cover glass is used in order to attain high quality fluorescence images while meeting the short working distance required by high-magnification oil immersion objectives. The glass is glued to a recess within a larger PEEK plate that serves as a frame, both supporting the glass and creating lanes in which independent experiments can be performed (Figure 2.3). Cover glass is cleaned by immersion in sodium hydroxide and sterilized in 100% ethanol prior to attachment with surgical grade silicone ATV.

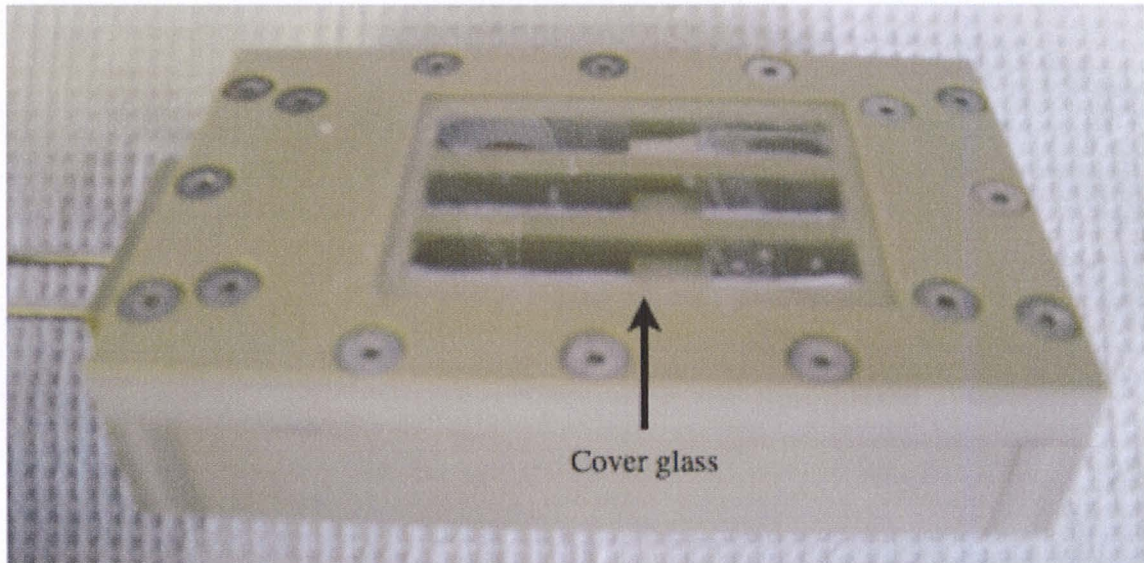


Figure 2.3 Cover glass viewing window.

2.3 Stretch-Growth

2.3.1 Culture Chamber Interior

Stretch-growth is performed by way of a towing mechanism. A portion of each glass well is covered by a thin 0.002" Aclar (highly flexible and translucent film) strip. The Aclar is pulled down the length of the chamber by a PEEK towing block that is fastened

to stainless steel towing rods extending outside the chamber. Axon stretch-growth occurs as the towing block separates populations of cells plated on the Aclar and glass (Figures 2.4 & 2.5). Similar to cover glass, the Aclar is cleaned by immersion in sodium hydroxide and sterilized in 100% ethanol prior to attachment to the towing block with surgical grade silicone ATV. The towing block and rods are sterilized by autoclaving.

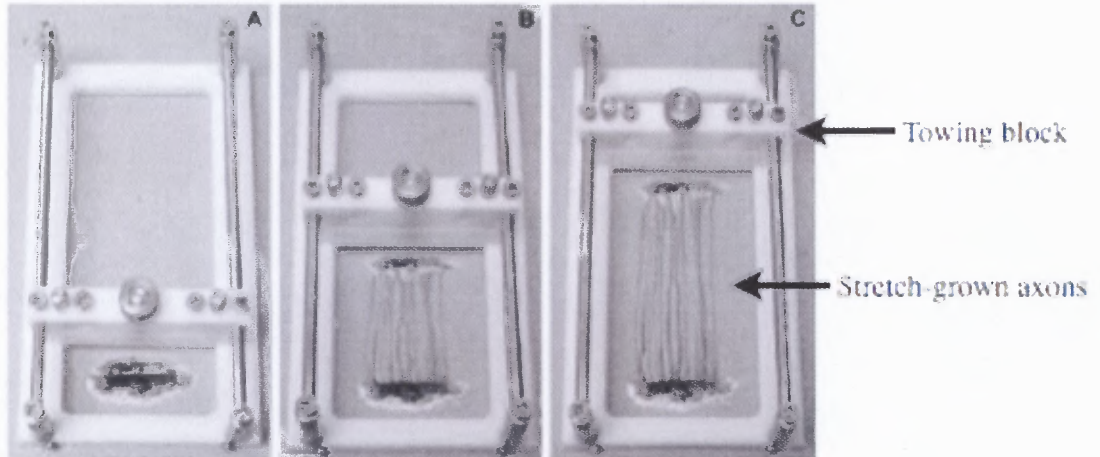


Figure 2.4 University of Pennsylvania extreme stretch-growth frame illustrating a single lane of stretch-grown axons. (A) Starting position of towing block. (B) Stretch-grown axons visible. (C) Stretch-growth completed as towing block reaches limit of travel.

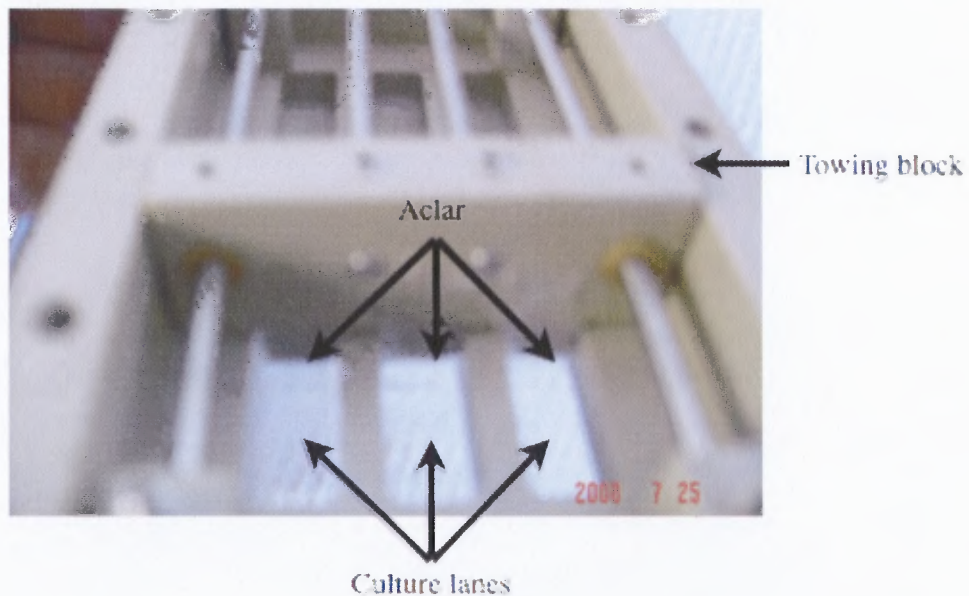


Figure 2.5 Live imaging stretch-growth bioreactor culture chamber. Three lanes visible, translucent Aclar strips attached to towing block and making contact with cover glass.

2.3.2 Culture Chamber Exterior

The towing mechanism can be immobilized as needed by engagement of a newly designed braking system built into the culture chamber. The towing rods extend through the PEEK braking block fastened to the outside of the culture chamber. Rubber braking balls housed in the block apply friction to the rods when compressed by external screws. During stretch-growth the compression is released by disengagement of the screws (Figure 2.6).

A computer-controlled linear motion table controls the extension of the rods out of the chamber (Figure 2.6). While the table allows for 2.66" of movement, the length of the cover glass limits the usable distance to roughly 2.5". A stepper motor from Servo Systems (Montville, NJ) provides driving force to the linear motion table (Figure 2.9). The step motor is powered by a drive controller (Si2035) from Applied Motion Products (Watsonville, CA) which connects to a PC via serial port. The controller is programmed using Si Programmer software from Applied Motion Products, running on Microsoft (Redmond, WA) Windows 2000 (Figure 2.7). The equipment is degreased and dusted; sterilization is unnecessary.

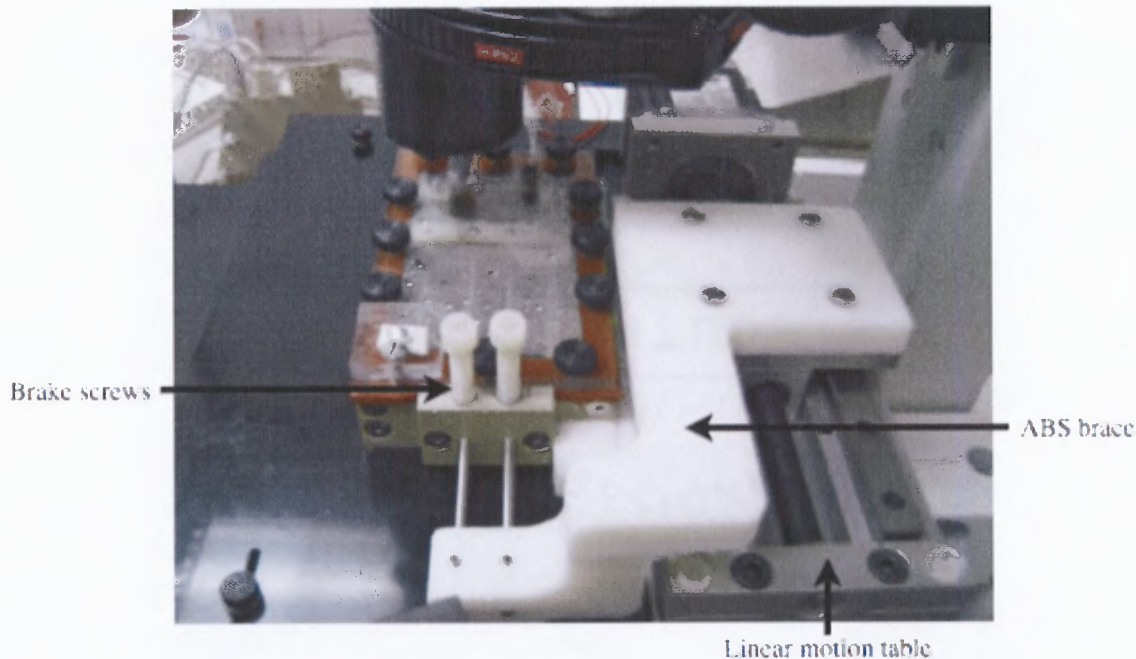


Figure 2.6 Exterior culture chamber stretch-growth components. Linear-motion table located behind the culture chamber interfaces with towing rods via ABS brace. External screws of braking mechanism shown disengaged.

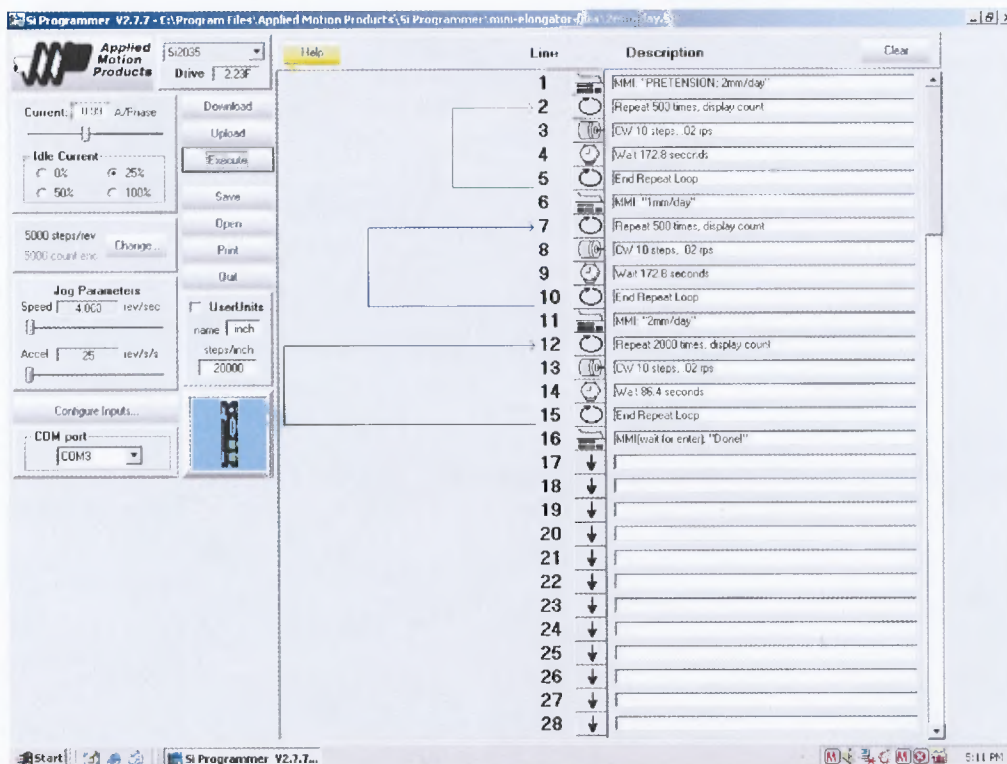


Figure 2.7 Screen-shot of SI Programmer controller software used for stretch-growth.

2.4 Gas and Humidity

A constant supply of pre-mixed gas containing 5% CO₂ and 95% O₂ is perfused through the culture chamber. A pressure regulator (valve size CGA 296) provides 5 psi of gas from a pre-mixed compressed air tank. A manifold containing an adjustable needle valve further reduces the pressure. From the manifold, the air is sterile filtered to 0.2µm before bubbling through a Fisher (Waltham, MA) diffuser stone (1" diameter, 60µm average pore size). The stone is immersed in sterilized culture grade water in a sealed 500mL Erlenmeyer flask; submerged in a 40°C water bath (Figure 2.8). The warmed and humidified air collects at the top of the flask and passes through two sterile filters in series (Figure 2.10) prior to perfusion through the culture chamber. A port built into the lid ducts the air approximately 1" above the cells. Air is allowed to escape at the rear of the culture chamber through a filter paper sealed port, see Figure 2.2 for port locations.

The sterile filters arranged in series allow disconnection of the culture chamber from the air system while maintaining sterility. The air tubing, connection ports and diffuser stone are autoclaved for sterility. Fresh sterile filters are used for each experiment.



Figure 2.8 Erlenmeyer flask within heated water-bath. Gas is bubbled through sterile water for humidification prior to filtration and perfusion into culture chamber.

2.5 Temperature

The culture chamber is warmed to physiological 37°C by an internal silicone heating element (HLS-8x.8p) from Cell MicroControls (Norfolk, VA). The heating element is positioned approximately 1” behind the stationary population of plated cells in order to avoid overheating of the cells and interference with the towing block. A metal thermistor probe mounted in the lid, above the cells, provides temperature feedback (Figure 2.2). The heating element and thermistor are controlled by a programmable temperature controller (mTCII) from Cell MicroControls as shown in Figure 2.10. The heating element and thermistor are immersed in sodium hydroxide overnight for sterilization.

2.6 Mounting and Plumbing

The culture chamber and linear motion table are aligned in parallel atop the microscope stage by a Delrin plastic chassis (Figure 2.9). The chassis affixes the stage, culture chamber, and linear motion table such that they cannot be moved independently. The center of the chassis is hollowed such that the culture chamber can sit flush on the microscope stage. ABS plastic braces fabricated on a 3D printer further steady the culture chamber and align it precisely in place. Another ABS brace fastens the towing rods to the linear motion table as shown in Figure 2.6. The equipment is degreased and dusted; sterilization is unnecessary.

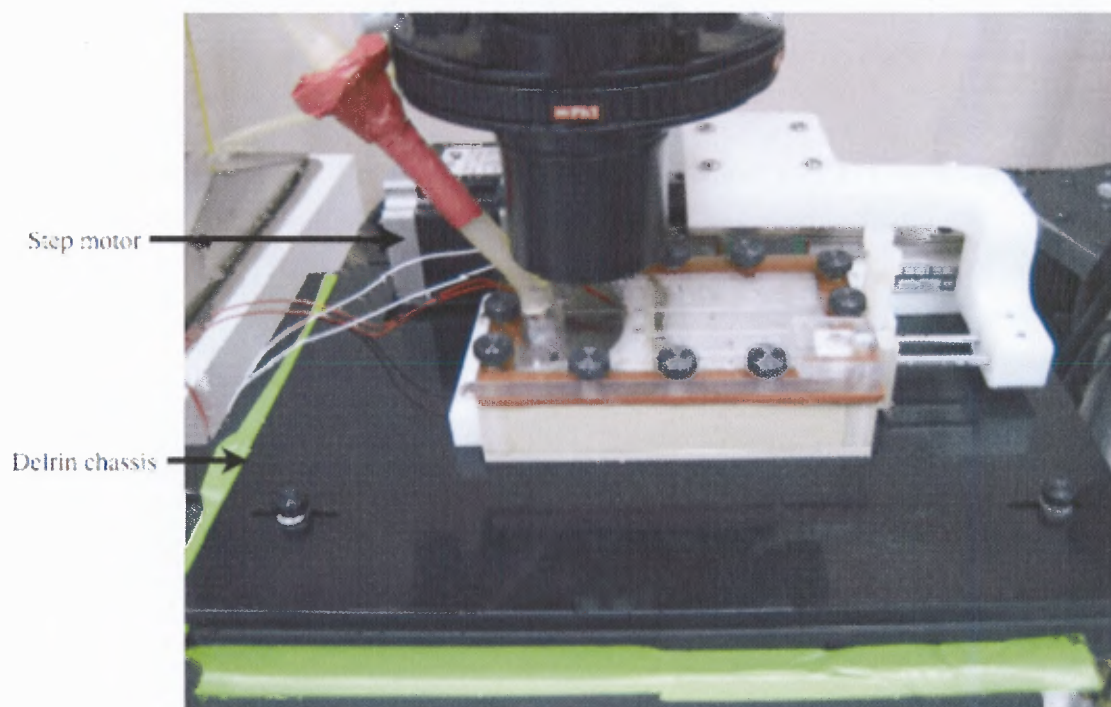


Figure 2.9 Live imaging stretch-growth bioreactor atop delrin chassis, affixed to inverted microscope stage.

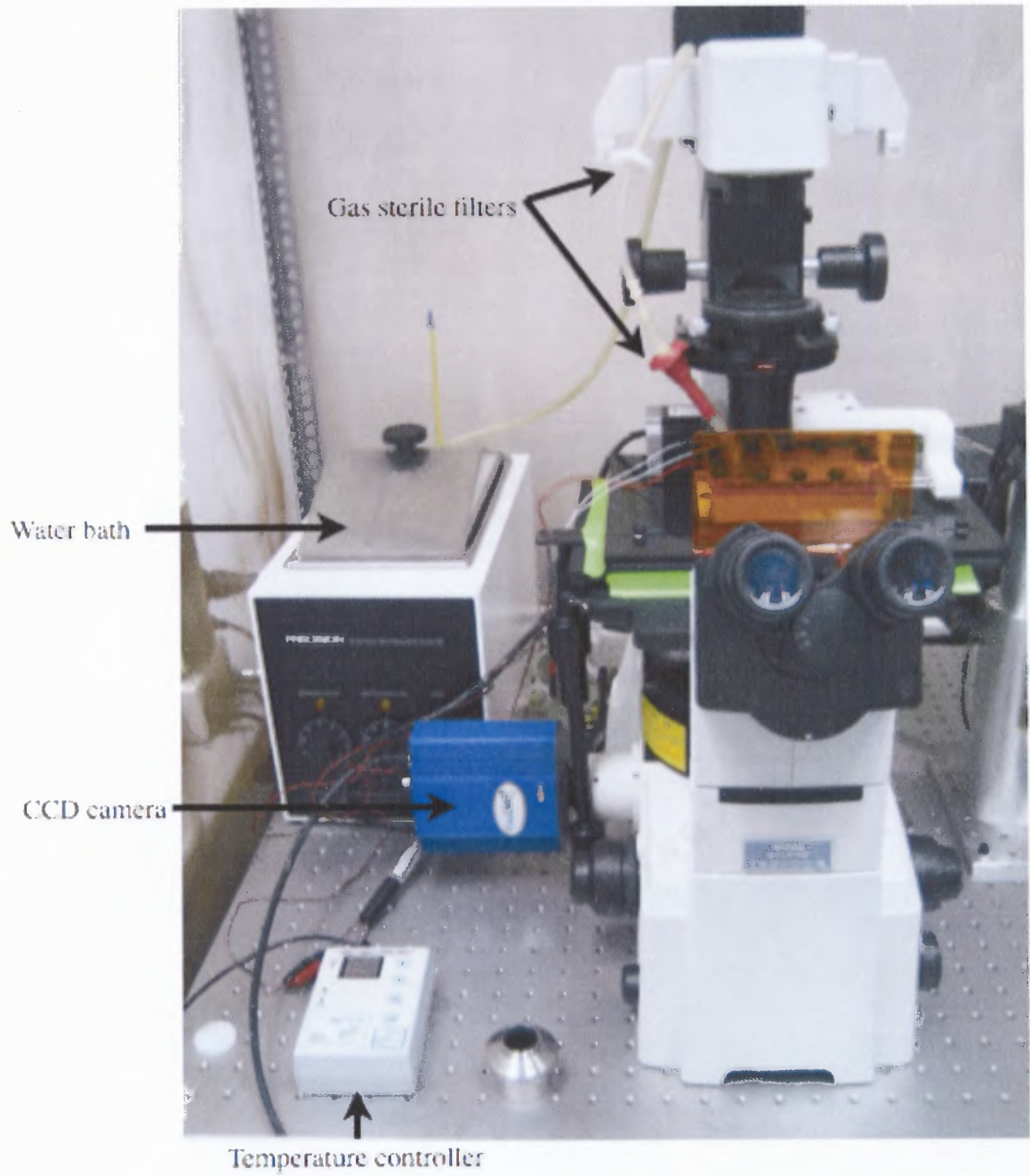


Figure 2.10 Complete live imaging stretch-growth system.

CHAPTER 3

DESIGN OF STRETCH-GROWTH GENE EXPRESSION EXPERIMENT

To facilitate understanding of the genetic regulation of axon stretch-growth, the RNA species active during this process were isolated and compared to non-stretch-grown controls. In order to generate sufficient quantity of RNA for downstream analysis, stretch-grown tissue was grown *in vitro* as previously reported by Pfister et al. [12] using bioreactors developed at the University of Pennsylvania (Figure 3.1). The tissue was dissected using a protocol adapted from B.J. Pfister (originally used to isolate protein) for the isolation of RNA. Non-stretch-grown controls were grown *in vitro* using 80mm petri dishes coated with Poly-L-Lysine (PLL) and type-1 rat-tail collagen in order to mimic coating of the Aclar as used in stretch-growth. A minimum of 100ng RNA was needed from both sample types in order to perform downstream DNA microarray analysis.

To promote upregulation of stretch-growth genes, the stretch rate was optimized to provide the highest possible growth rate while minimizing axon disconnection. While most axons do undergo stretch-growth, there are some axons that disconnect during the *in vitro* process. It was assumed that such disconnection would lead to the expression of stress-response genes. Activation of a variable, competing, genetic response was undesirable since it would likely lead to unfavorably skewing of the data.

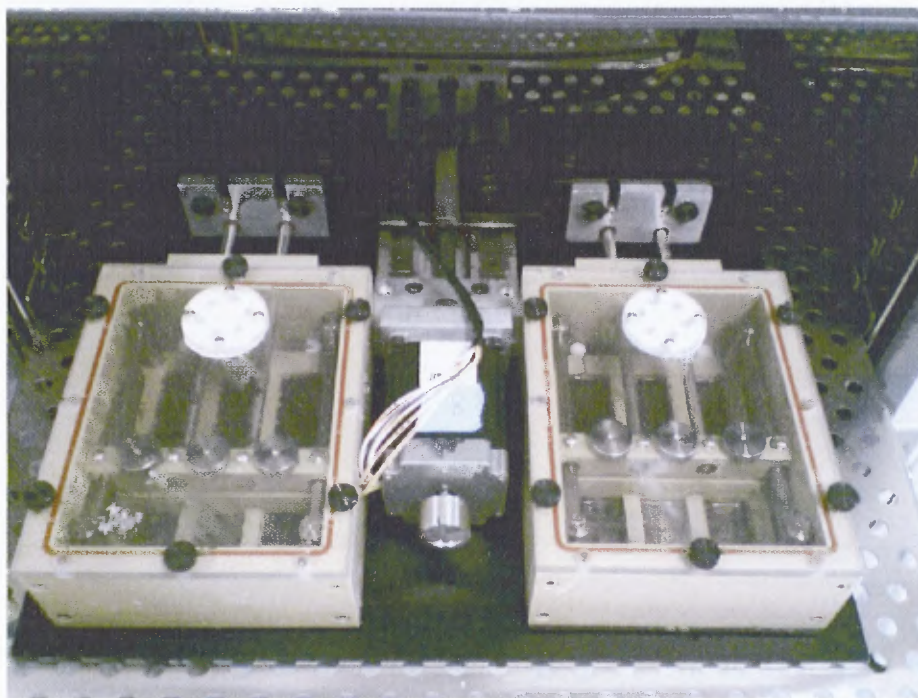


Figure 3.1 Stretch-growth bioreactors developed at the University of Pennsylvania.

In order to obtain statistically significant results, three experiments were repeated for DNA microarray analysis. The generation of tissue was done in a highly controlled and reproducible fashion between experiments. For each experiment, stretch-grown and non-stretch-grown-controls were cultured from the same homogenized pool of DRGs collected from the embryonic rat pups of a single mother. Due to genetic variation between individual rat pups, pooling all DRGs before plating was expected to result in more equivalent comparison of the resulting RNA species isolated from stretch-grown and non-stretch-grown controls. Furthermore, in order to reduce variability between experiments, a consistent number of embryonic rat pups were dissected throughout all experiments during isolation of DRGs.

Quantification of collected RNA from stretch-grown samples was compared to that of non-stretch grown control samples. Collected RNA was quantified on a NanoDrop (Thermo Scientific, Waltham MA), a highly sensitive spectrophotometer requiring less than 2ul of sample volume. Averages and standard deviations were calculated and compared across multiple experiments.

Gel electrophoresis (1% agarose gel) was used to assess quality of the RNA (appendix F). Samples were deemed good quality if distinct 16S and 28S ribosomal RNA bands were visible, whereas additional bands or smearing indicated degraded RNA. In future experiments, samples of adequate quantity and quality will be amplified, labeled, and hybridized to DNA microarrays. The chips will be scanned using a laser scanner and analyzed. Non-stretch-grown control data will be compared to experimental stretch-grown data in order to reveal the identity of genes associated with stretch-growth [14].

CHAPTER 4

RESULTS

4.1 Live Imaging Stretch-Growth Bioreactor

Following construction of the bioreactor, each sub-system was individually tested prior to *in vitro* culturing. Further testing of the complete system *in vitro* identified necessary changes of the initial protocols and methods. The following sections provide comprehensive results of the protocols and methods that were successfully tested for each sub-system of the live imaging stretch-growth bioreactor.

4.1.1 Experimental Protocol

All components of the bioreactor requiring autoclave sterilization were autoclaved on the Friday of the week prior to the scheduled plating. Autoclaved components were allowed to dry thoroughly in a sterile hood over the weekend. The remaining components requiring sterilization were immersed in 1N sodium hydroxide solution on Friday. Continuing from this point, the assembly and preparation was done in a sterile hood in order to prevent subsequent experiment contamination.

On Monday the cover glass and Aclar were rinsed twice in purified and sterilized water and then again in 100% ethanol to facilitate drying. A sterilized box of pipette tips was used as a drying rack. While the substrates were drying, the bottom of the PEEK stretching frame was lightly covered with surgical grade silicone ATV applied with sterile cotton-tipped swabs. The cover glass was gently placed against the bottom of the stretching frame and gentle pressure was applied using cotton-tipped swabs in order to push out trapped air. Next, the Aclar was cut into thin strips approximately 25mm long

by 5mm wide using dissecting scissors. The towing block was coated with glue and the Aclar strips were applied against the block with the sanded edge curving down into the culture well overlapping the cover glass by approximately 1mm. The culture box was then exposed to UV light while remaining in the hood over two days to allow curing and cross-linking of the glue.

Wednesday, the lanes were filled with 2% 3-aminopropyltriethoxysilane/acetone (APES) solution for two minutes. The lanes were drained and air-dried for ten minutes prior to coating of the glass and Aclar plating area with 20ul type-1 rat-tail collagen. Ammonia vapors were used to promote polymerization and cross-linking of the applied collagen.

DRGs from one embryonic rat pup were isolated according to the protocol outlined in appendix A. Cells were plated on the cover glass and Aclar substrate approximately 100 μ m apart using the DRG plating method as outlined in appendix B. An incubation period of five days allowed growing axons to synapse across the two populations of cells in a conventional incubator.

After the incubation period, the delrin chassis and linear motion table were fastened to the microscope stage. The water bath was brought to 40°C and gas flow was initiated. The culture chamber was fitted to the stage and connected to the heating controller and gas port. With the external brake of the culture chamber engaged, the alignment of the linear motion table and culture chamber was test fitted with the ABS brace. The position of the linear motion table was adjusted using Si Programmer to increment the position as needed. Once in alignment, the ABS brace was tightened in place and the brake on the culture chamber was released. Stretch-growth of axons was

initiated at 1mm/day and increased to 2mm/day according to the program schedule in appendix D.

4.1.2 Culture Chamber

Cells were cultured for up to two weeks utilizing conventional incubators prior to experimentation on the microscope stage. Media was changed every two to three days within a sterile hood in order to prevent contamination. Cells were later cultured for six days on the stage of the microscope with the same media change intervals (see appendix C). Sterility was maintained throughout this time.

4.1.3 Viewing Window

Despite careful handling, the viewing window was easily broken during cleaning and gluing. A spare cover glass was prepared simultaneously in case this occurred. Unused spares could not be used since they turned opaque when left in the sodium hydroxide solution for prolonged periods. Once glued in place, the viewing window never leaked and was able to withstand the force exerted by oil immersion objectives without cracking.

4.1.4 Temperature

Upon initial heating, the temperature was shown to exceed and eventually return to the temperature set on the controller as shown in Figure 4.1. Although the temperature only reached a maximum of 40°C as recorded at the thermistor, a maximum of 68°C was recorded on the exterior of the culture chamber by an infrared thermometer. Such temperatures are lethal to cells and could also result in degradation of the media and coatings. To avoid this, the culture chamber was always pre-warmed in a conventional incubator prior to experimentation on the microscope stage. Upon removal from the

incubator, the culture chamber temperature was successfully maintained by the internal heating element. Operation in a temperature-controlled room with ambient temperature of 23°C limited the temperature fluctuation inside the culture chamber to within a 2°C range of 37°C for three days.

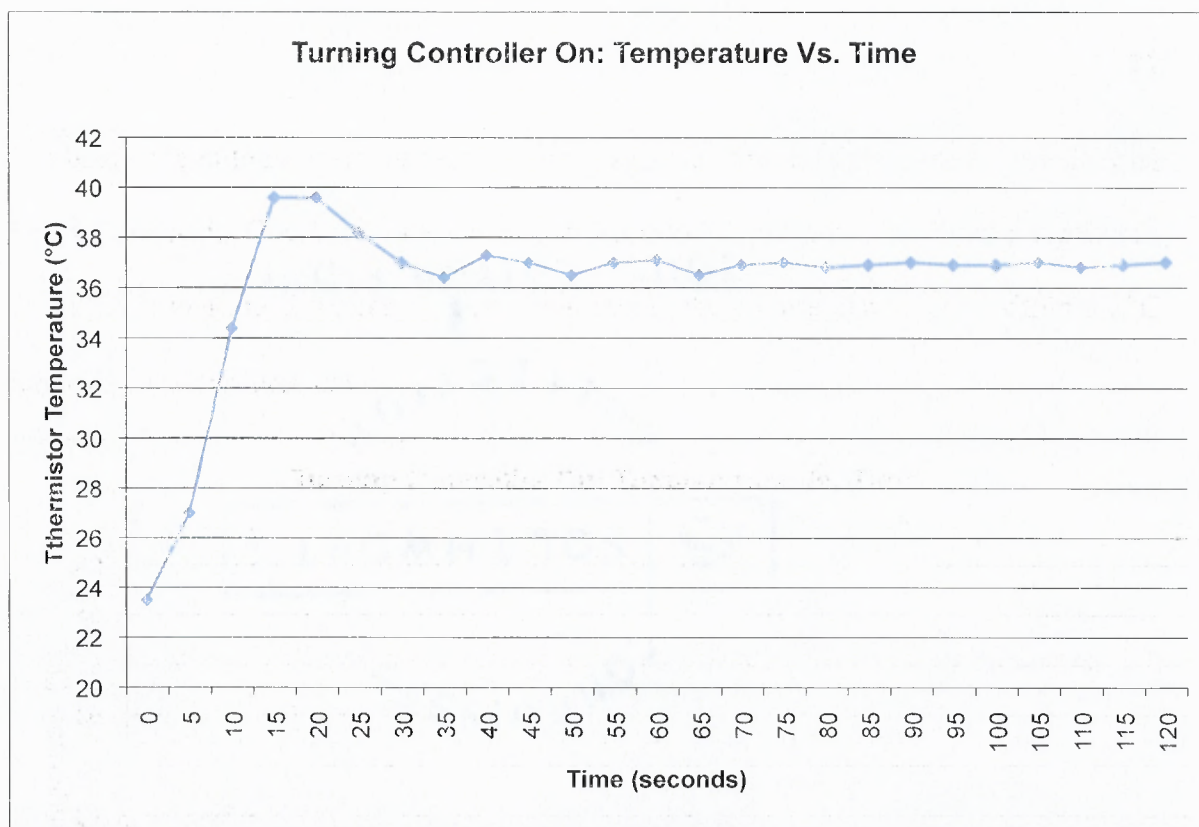


Figure 4.1 Temperature controller overrun upon initial heating from room temperature. Temperature was read from thermistor located within culture chamber lid above plated cells.

4.1.5 Gas and Humidity

In order to maintain the culture media at physiological pH beyond 24 hours, the flow of gas containing CO₂ needed to be maintained by periodic adjustment. Pressure from the regulator needed to be periodically raised in order to maintain pressure of 5 psi out of the air tank. Left unattended, the regulator would drop to undesirable pressure levels within two days time, resulting in higher pH of the culture media and complete cell death. To

correct this, it is planned to test higher pressures from the regulator and reduced at the manifold with the needle valve, allowing the system to go unattended for longer periods.

Sterile filters had to be relocated further away from the water bath. Water condensed inside the tubing and was pushed into the filters by the flow of air. The sterile filters would no longer pass air after wetting, which necessitated replacement. Relocation of the filters to a higher location away from the water bath prevented reoccurrence of wetting.

4.1.6 Stretch-Growth

Stretch-grown axons were grown at up to 2mm/day on the stage of the microscope for several days. Higher stretch rates were not attempted since it was desired to test how long the existing axons could be maintained. Future experiments will increase stretch rates up to 6mm/day.

4.1.7 Mounting and Plumbing

One issue identified during experimentation will be corrected before performing additional experiments. The gas inlet tubing interfered with the overhead light source of the microscope, as can be seen in Figure 2.9. The obstruction prohibited positioning of the microscope stage and subsequent imaging of the culture within a radius of approximately 5mm from the port. A 90° angled port will replace the current port to alleviate the interference.

4.1.8 Bright Field Live Imaging

Stretch-grown nervous tissue was successfully grown and captured live on the stage of a Nikon TE2000-S inverted microscope. Magnification ranges from 40x to 600x provided high quality still images of the stretch-growth process as shown by Figures 4.2, 4.3, 4.4, 4.5.

Voodoo time-lapse software by Photometrics (Tucson, AZ) was used to record the changes in morphology over 17 hours of stretch-growth. Still images were taken in five-minute intervals, producing sequences of 204 images (Figure 4.6). It is possible that additional images could be taken over shorter intervals and longer periods with additional PC RAM. Focus of time-lapse imaging was not optimal throughout the experiment since the tissue in view was in motion and needed periodic refocusing.

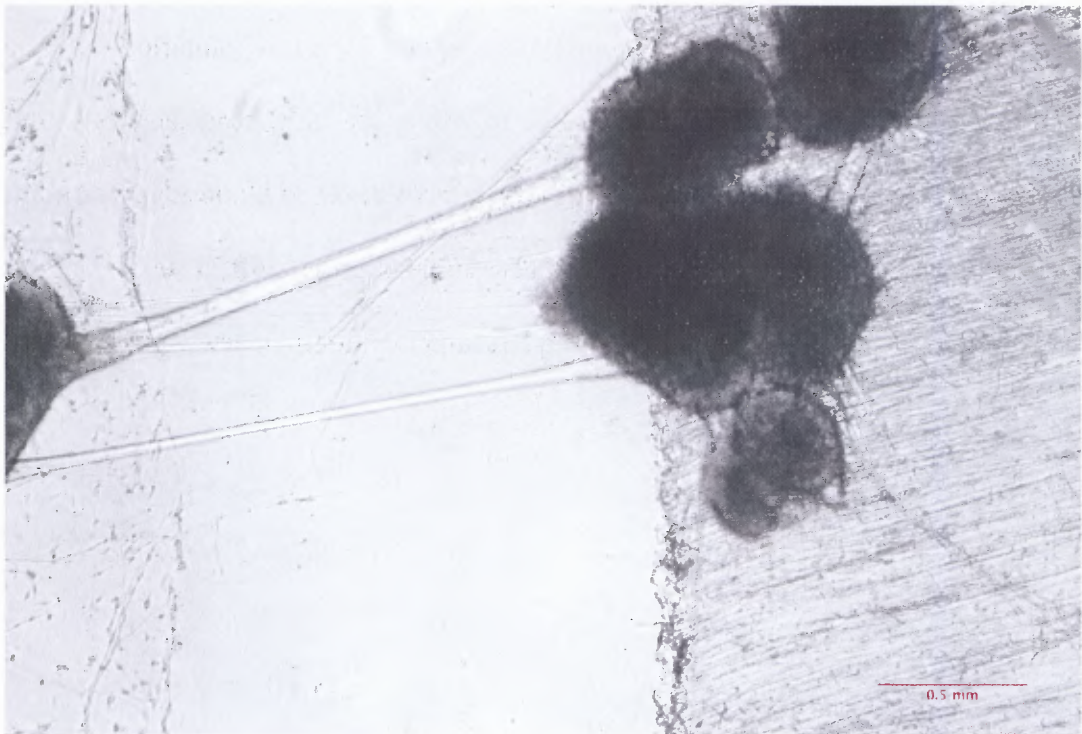


Figure 4.2 Stretch-grown axons shown utilizing 4x objective. Bar = 500 μ m.

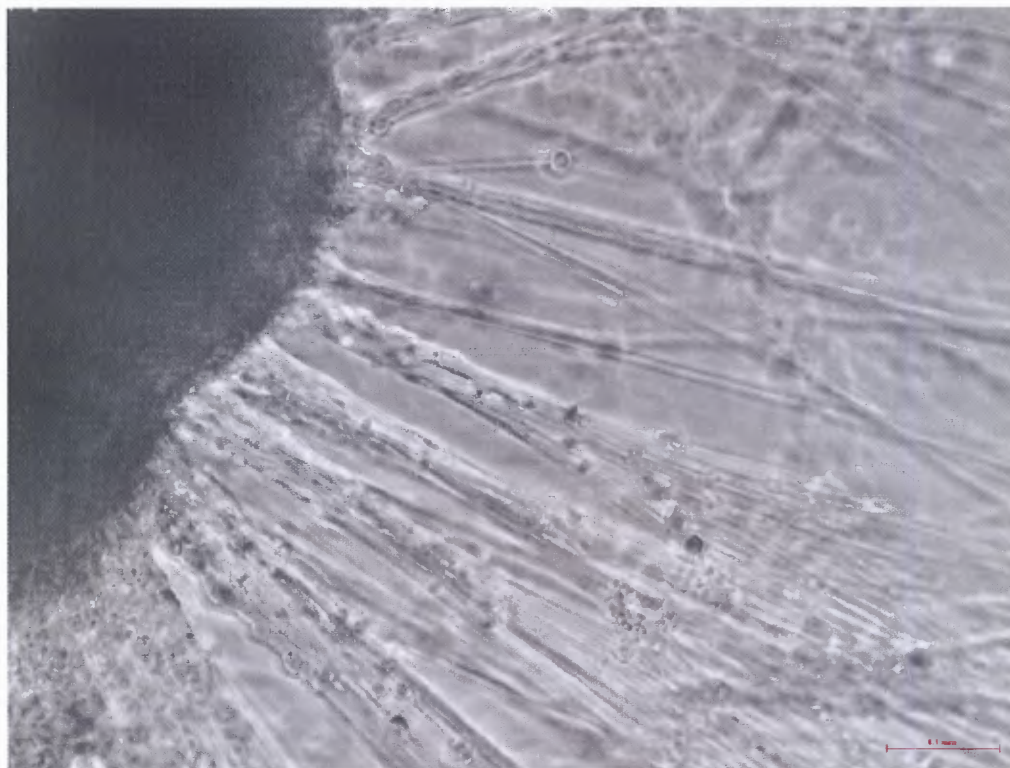


Figure 4.3 Stretch-grown axons shown utilizing 10x objective. Bar = 100 μ m.

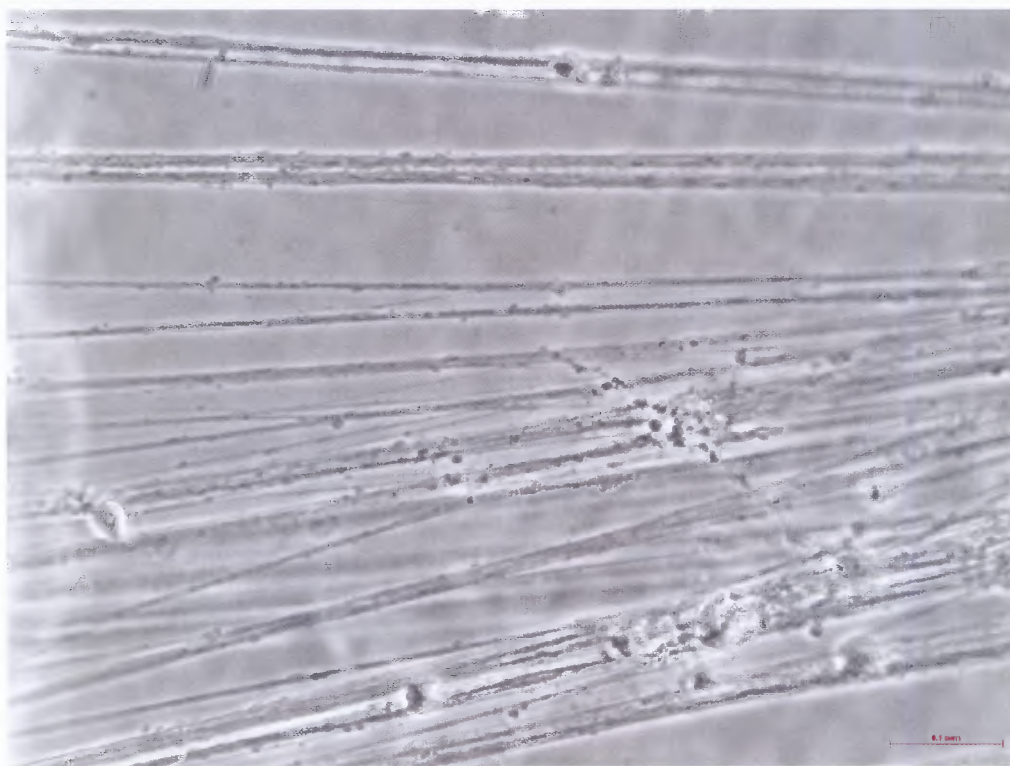


Figure 4.4 Stretch-grown axons shown utilizing 10x objective. Bar = 100 μ m.

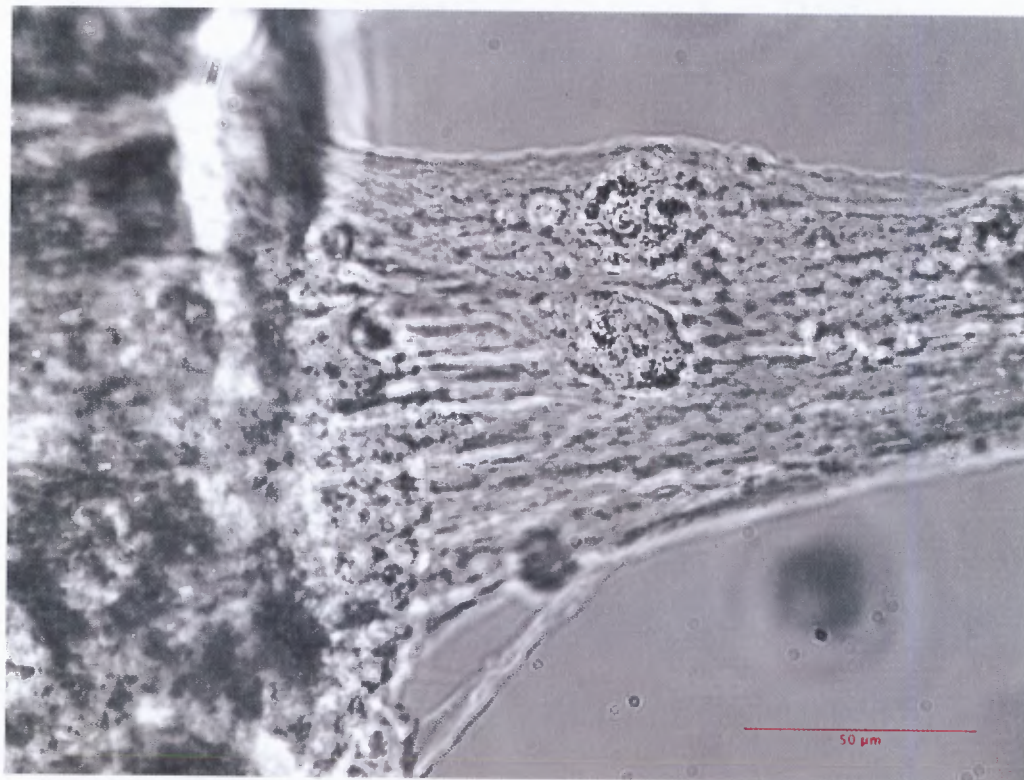


Figure 4.5 Stretch-grown axons shown utilizing 60x objective. Bar = 50μm.

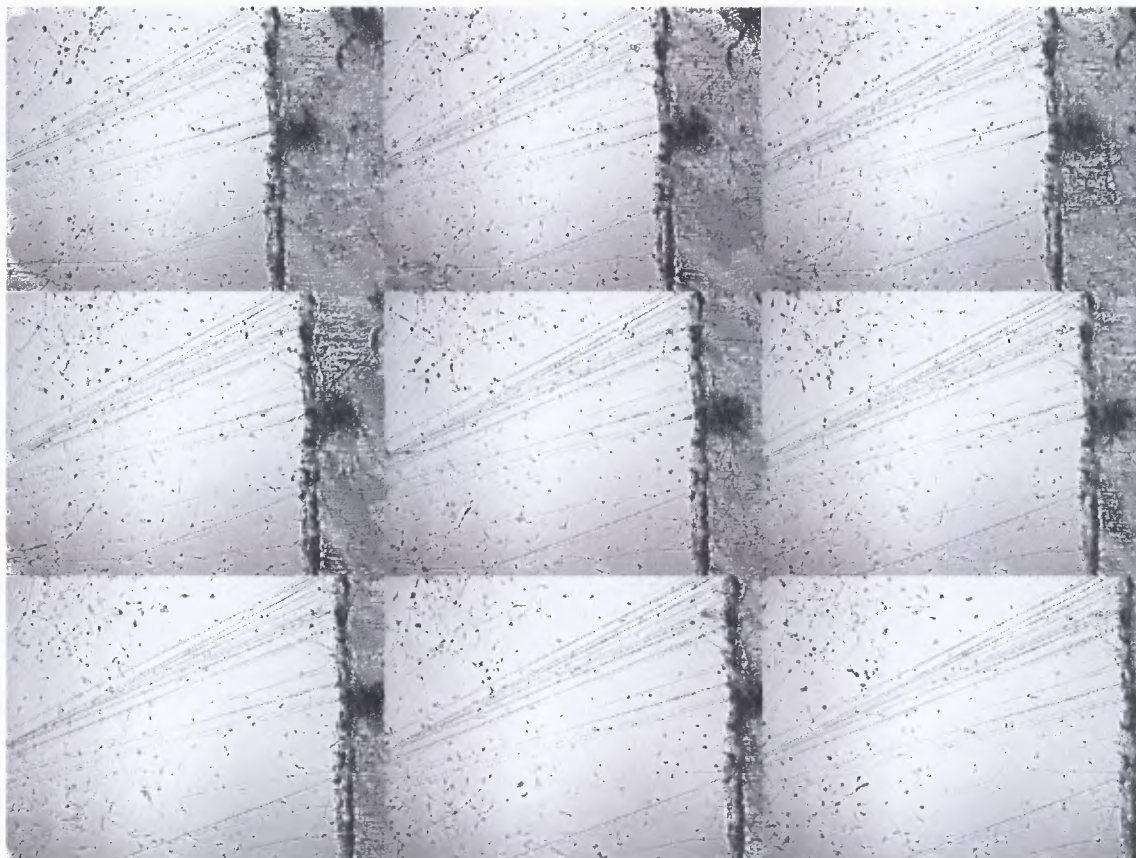


Figure 4.6 Stretch-grown axon live imaging time-lapse shown utilizing 4x objective. Montage represents 14 hours of stretching with 1.5 hours between frames as recorded by Voodoo time-lapse software. Stretch rate of 2mm/day recorded over 1.2mm of stretch-growth. Aclar towing substrate can be seen moving outside field of view toward right edge.

4.1.9 Fluorescence Live Imaging

In order to test the ability to track organelles that migrate from the cell body into the axon, mitochondria were stained and visualized in stretch-grown axons. MitoTracker Red from Invitrogen Corporation (Carlsbad, CA) was used to stain actively stretch-growing axons following the protocols used to stain non-stretch-grown axons by Dr. Kyle Miller, Department of Zoology, Michigan State University [9]. Briefly, stretch-grown axons were stained for one minute in 100 nM MitoTracker Red dye and rinsed with Phosphate Buffered Saline (PBS). After incubation for thirty minutes, mitochondria were

visualized on a Nikon TE2000-E confocal microscope at 600x using an oil immersion objective. Imaging was facilitated by removal of culture media in order to reduce floatation and improve focus of stretch-grown axons.

It was found that stretch-grown axons contain abundant mitochondria, see Figure 4.7. A Z-stack of 15 μ m with a step size of 3 μ m was taken in order to observe intra-axonal mitochondria within multiple planes, see Figure 4.8. Due to the tendency of stretch-grown axons to form thick bundles, visualization of individual intra-axonal mitochondria was not observable. Quantification and transport of mitochondria within individual stretch-grown axons may be facilitated by plating fewer DRGs or by dissociating DRG explants prior to plating.

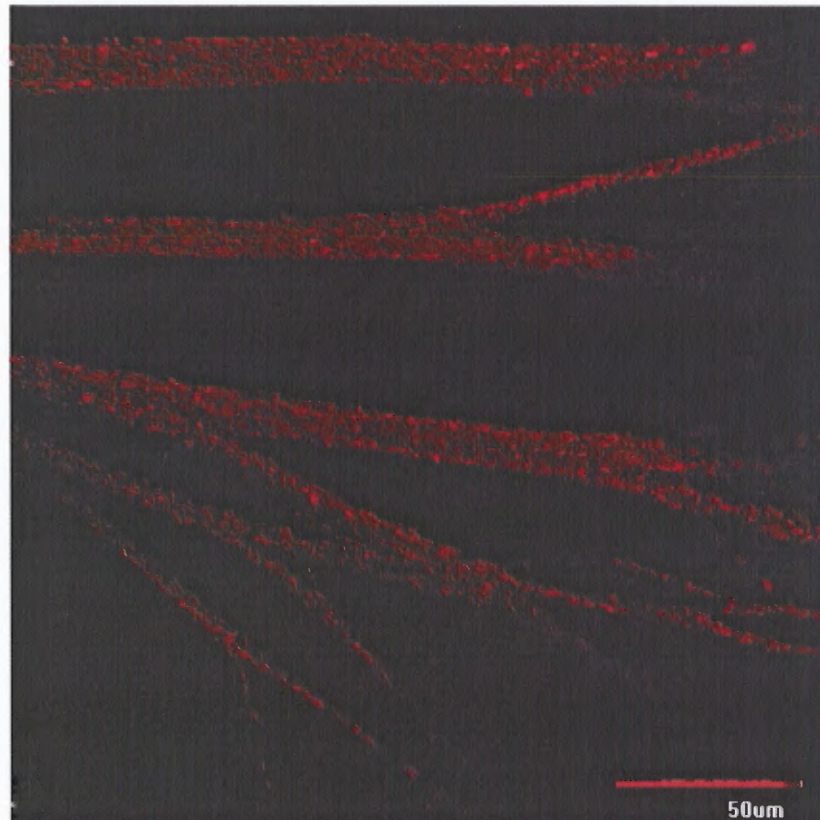


Figure 4.7 Stretch-grown axons stained for mitochondria, confocal microscopy shown utilizing 60x objective. Bar = 50 μ m.

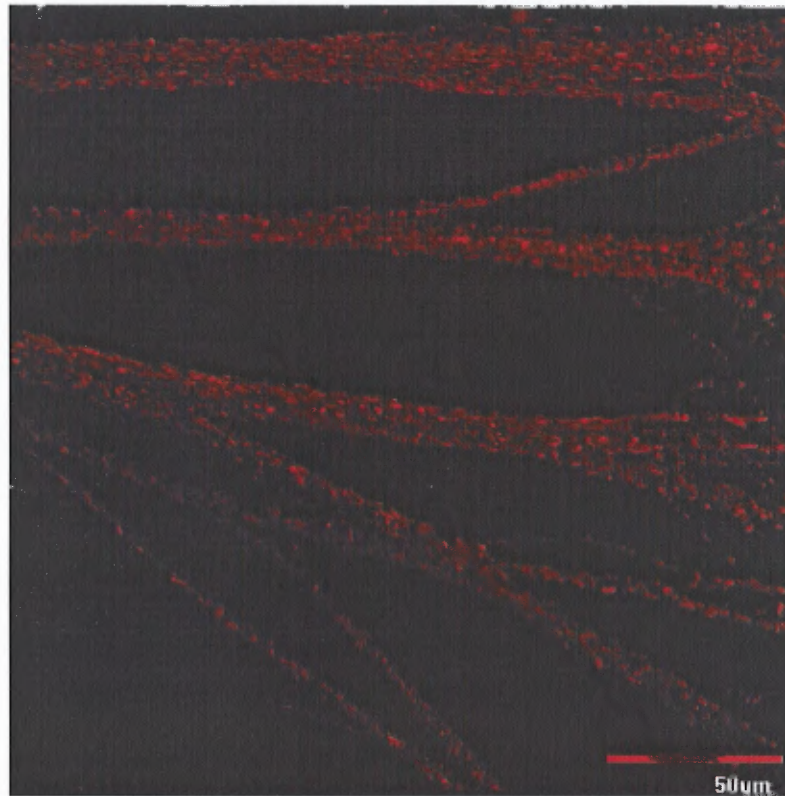


Figure 4.8 15µm Z-Stack volume render of stretch-grown axons stained for mitochondria, confocal microscopy shown utilizing 60x objective. Bar = 50µm.

4.2 Stretch-Growth Gene Expression

The following sections provide comprehensive results of the protocols and methods that were used for *in vitro* growth, isolation, and analysis of stretch-grown and non-stretch-grown associated gene expression.

4.2.1 Growth of Tissue and Isolation of RNA

Isolations of primary DRGs from embryonic rat pups consistently yielded a minimum litter of 12 pups from each pregnant rat. In order to maintain consistency between experiments, no more than 12 pups were dissected for DRGs despite larger litters. The DRGs from all 12 pups were pooled in a single microcentrifuge tube during isolation.

Stretch-grown and non-stretch-grown control tissues were cultured simultaneously and treated to the same media change intervals and incubation conditions (9% CO₂, 37.0°C). Stretch-grown tissue was grown as previously described by Pfister et al. [12] with two primary differences. First, the stationary Aclar bottom originally used was replaced by thinner 0.002" Aclar. Utilization of the original Aclar resulted in inconsistent adhesion of the stationary cells, as shown in Figure 4.9. By switching to thinner Aclar, as was used for the towing substrate, adhesion inconsistencies were eliminated and DRGs remained adhered during experiments (Figure 4.10). Additionally, the thinner Aclar facilitated dissection of stretch-grown tissue for subsequent RNA isolation. Second, the stretch-growth rate was optimized to prevent inconsistent disconnection of axons during stretch-growth. The stretch rate was eventually limited to 6mm/day, a reduction from the maximum of 10mm/day previously achieved by Pfister et al. At 8mm/day or faster, stretch-grown axons sporadically disconnected and degenerated, resulting in inconsistent amounts of tissue. When grown at 6mm/day, more consistent bundles of axons could be visually observed with little disconnection or degeneration.

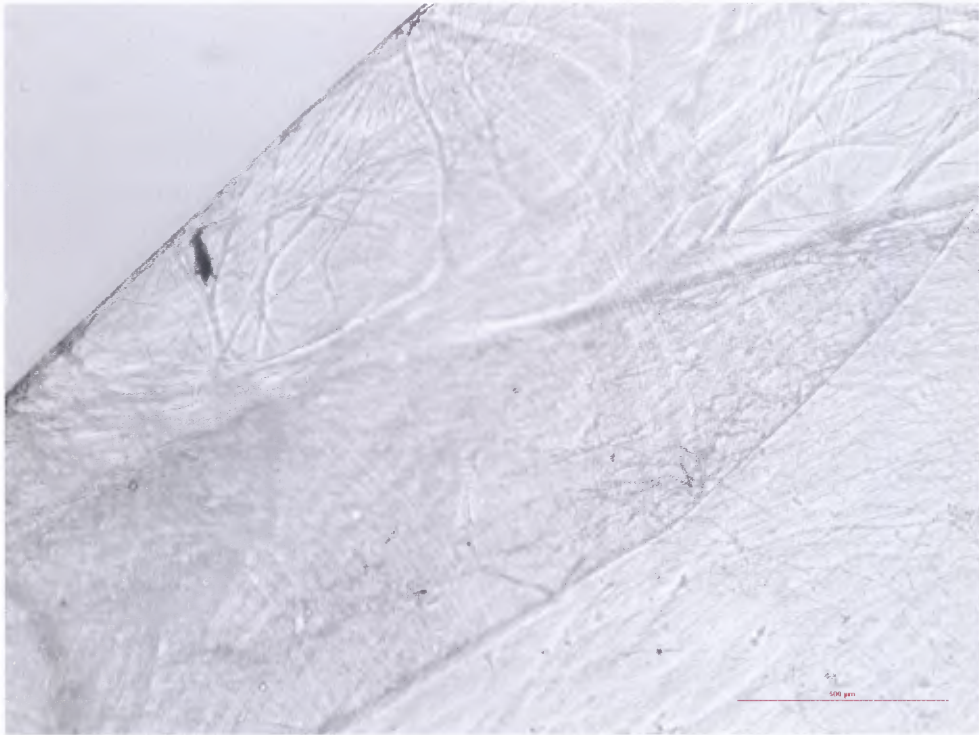


Figure 4.9 Aclar coating failure. Upper left corner shows peeling of stretch-grown axons away from the Aclar originally used in stretch-growth. Bar = 500 μ m.



Figure 4.10 Stretch-grown axons. Aclar towing substrate visible along right edge. Bar = 500 μ m.

Once stretch-growth reached the desired stretch rate of 6mm/day, stretch-growth was continued for an additional 24-hours. It was hypothesized that allowing one day's time to pass at the target growth rate would ensure consistent expression of genes required by stretch-growth. During the last two hours of stretch-growth, the materials and tools necessary for RNA isolation were prepared. Dry ice was used to fill the lid of a Styrofoam container, creating an ice-like surface on which to keep the tissue frozen during dissection. Pipettes and dissection tools were treated with RNase-Zap, eliminating potential contamination with RNA-degrading substances such as oil released through the skin. The dissecting scalpel, tweezers and fine scissors were covered with dry ice until the isolation began.

Working quickly after stretch-growth, the culture media was removed from the lanes within the incubator in order to minimize trauma to the axons during transport. Visualization at 40x was performed in order to verify the consistency of the tissue in each lane. Lanes with excessive disconnection of tissue were excluded from RNA isolation. The stretching frame with tissue was removed from the reactor box and remaining media was aspirated. The stretching frame and tissue were frozen on dry ice for ten minutes to preserve the active RNA species while facilitating the removal of the tissue from the frame. Working one lane at a time using a scalpel, the tissue and Aclar within the stretching frame were cut out in a single piece. The stretching frame was placed back on dry ice with the uncut lanes while the removed tissue was further dissected. Using scissors, the tissue and Aclar were cut horizontally across the stretch-grown axons (including soma) into thin strips no larger than 4mm wide. The thin strips were immediately placed into the bottom of a 15ml centrifuge tube containing 1ml of ice-cold

lysis buffer. Each lane was successively dissected and added to the same tube. Once all tissue was collected, the tube was warmed using the palm of the hand for 30 seconds, then vortexed for 90 seconds. 1ml of 70% ethanol was added and mixed with the sample by pipette. The lysed liquid sample was then loaded onto Qiagen (Valencia, CA) RNeasy columns while leaving the Aclar strips behind in the tube. The protocol as provided with the RNeasy kit was followed from this point as outlined in appendix E from step #5.

Two petri dishes of non-stretch-grown controls (Figure 4.11) were isolated for RNA immediately following isolation of RNA from stretch-grown tissue. Each plate was individually aspirated of media and frozen on dry ice for five minutes to mimic the isolation of RNA from stretch-grown tissue. The dish was then placed on wet ice with 1ml of lysis buffer and washed frequently with the buffer in order to disrupt attachment of cells. After five minutes, the lysis buffer was removed and reused for the next plate of controls. The collected lysate was briefly warmed in the palm and vortexed in a 15ml centrifuge tube prior to mixing with one volume 70% ethanol. The protocol as provided with the RNeasy kit was followed from this point as outlined in appendix F from step #5.

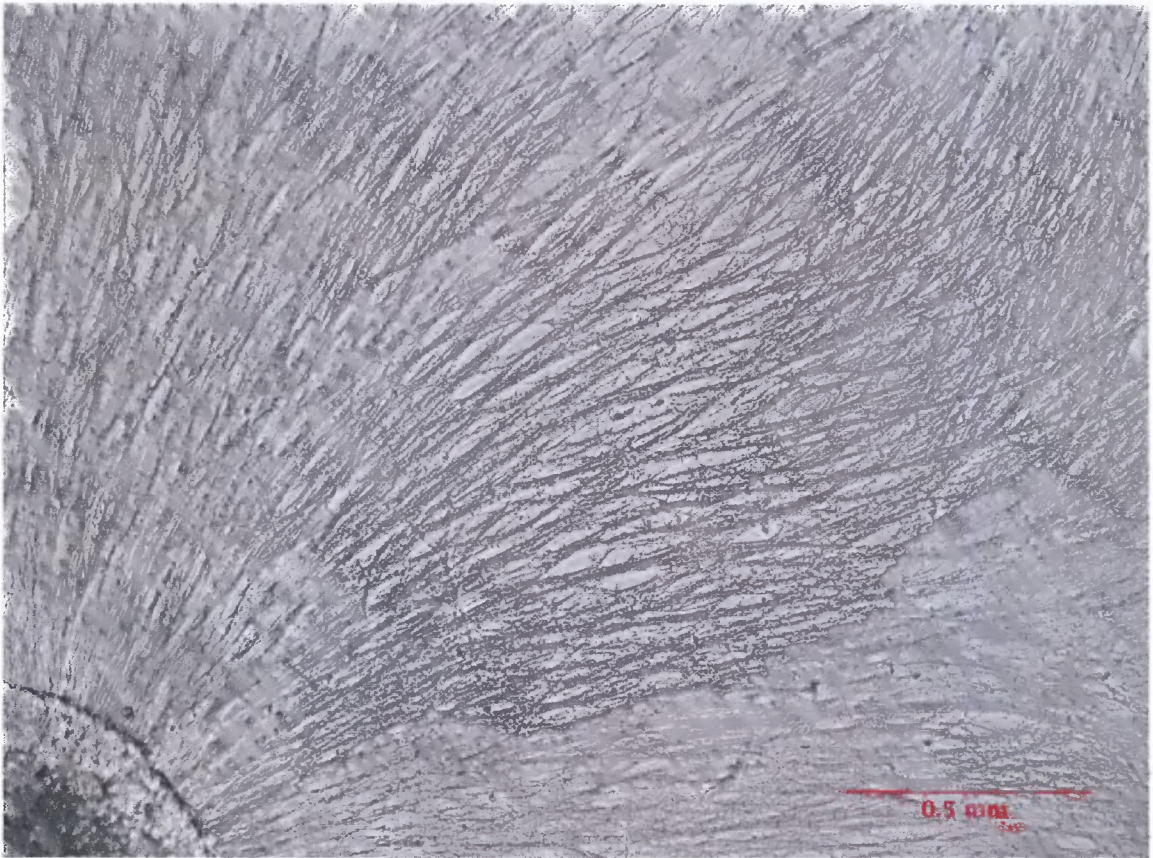


Figure 4.11 Non-stretch-grown controls. Bar = 500 μ m.

4.2.2 Quantification and Visualization of RNA

Total RNA as isolated with the RNeasy kit was quantified on the Nanodrop UV Spectrophotometer. Six experiments produced an average of 7,073ng RNA with a standard deviation of 4,924ng for non-stretch-grown control samples. Stretch-grown samples produced an average of 14,084ng RNA with a standard deviation of 4,367ng. Two experiments, X and Y, each excluded one of three lanes during RNA isolation from stretch-grown samples. Experiment U was the only unexplained outlier with 16,137ng from the control sample, over double the average and almost double the standard deviation, see table 4.1 for detailed results.

Table 4.1 RNA Quantification

Expt	Control (ng)	6mm/day Stretch-Grown (ng)	Pups	Days	Comment
Q	4,620	18,000	12	13	
R	4,380	17,280	12	13	
U	16,137	9,807	12	13	Outlier
W	4,140	18,615	12	12	
X	3,687	11,787	12	12	2/3 lanes
Y	9,471	9,015	12	12	2/3 lanes

It was thought that a higher stretch rate would result in a broader difference between sample types. Early isolation of stretch-grown tissue at stretch rates of 8mm/day or faster resulted in inconsistent quantities of tissue collected (data not shown). This was observable under the microscope as well as by quantification of RNA. Early stretch-grown samples at 8mm/day or faster produced an average of 6,712ng, less than half the amount isolated from tissue stretch-grown at a slower 6mm/day (14,084ng).

A 1% agarose gel was run in order to visualize the quality of select RNA samples. The gel was prepared and run according to the protocols outlined in appendix F. The visual observation of sharp 16S and 28S ribosomal RNA bands without fragmentation or smearing indicated that collected samples were of high quality, ready for further downstream applications. The gel shown in figure 4.12 was run on early samples not included in table 4.1. Subsequent samples all produced equally high-quality results, suggesting the isolation methods worked reliably.

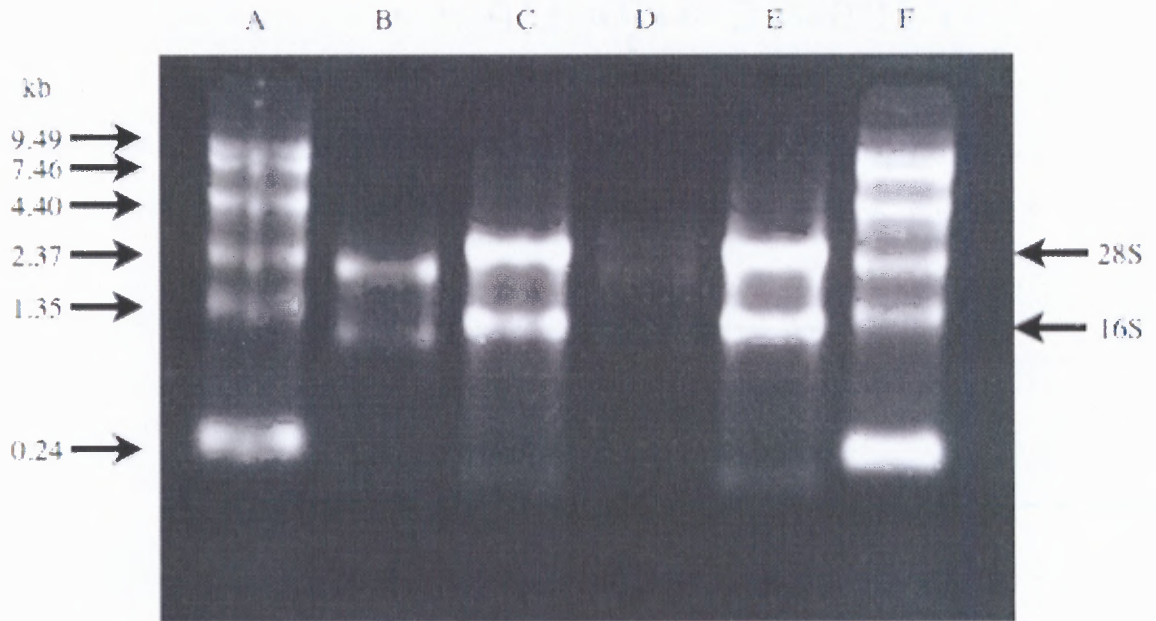


Figure 4.12 Gel electrophoresis of RNA stained with ethidium bromide and visualized by UV light, samples run top to bottom. (A&F) Invitrogen 0.24-9.5 Kb RNA ladder. (B&E) Non-stretch-grown control tissue. (C) 10mm/day stretch-grown tissue soma. (D) 10mm/day stretch-grown tissue axon.

4.2.3 Microarray Analysis

The DNA microarray processing and analysis will be completed as part of planned Ph.D. work.

CHAPTER 5

DISCUSSION

5.1 Live Imaging Stretch-Growth Bioreactor

Mitochondria were labeled and imaged in stretch-grown axons as evidence that the transport of organelles from the soma to the axon could be visualized within the bioreactor. Dr. Kyle Miller from Michigan State University has tracked mitochondria extensively in non-stretch-grown axons and has agreed to help repeat the analysis in stretch-grown axons. Additional collaborations have been sought to facilitate labeling and tracking of RNA and protein from soma into stretch-grown axons. Molecular beacons previously designed by Dr. Sanjay Tiyagi from PHRI, may be used to transfect and label RNA species found to be upregulated during gene expression [16]. Such species of interest are expected to correspond to those previously found in axons such as beta-actin, peripherin, vimentin, gamma-tropomyosin-3 and cofilin-1 [19]. In addition, plasmids with green fluorescently labeled beta-tubulin will be used to transfect DRGs in culture in order to visualize the assembly of microtubules as originally reported by Bray [2].

The live imaging stretch-growth bioreactor will also be used to study the effects of experimental culture conditions and drugs on stretch-growth. Three independent lanes within which to culture and image stretch-growth allows for side-by-side comparison of experimental groups with stretch-grown controls.

Future fluorescence imaging will be performed with the addition of a thickening agent added to the media, such as the commonly used methylcellulose. It was thought

that by increasing the viscosity of the media, vibration and focusing issues could be improved without complete removal of media. The rate of axon outgrowth will be carefully monitored in the presence or absence of methylcellulose. It has previously been shown that growth cone growth excels in liquid and is inhibited by thick tissues. Utilization of a thickening agent may require increased incubation time to allow synapsing to occur before stretch-growth if used throughout experiments.

The currently unstudied process of axon stretch-growth may offer unique and significant contributions to our fundamental knowledge of nervous system development. The overall expectation of the live imaging stretch-growth bioreactor is to increase our fundamental knowledge of what occurs during this natural process. By adding to the currently known biology of nerve growth and regeneration, the chances of discovering methods to repair the nervous system are increased. If enough knowledge of stretch-growth can be garnered, the process could be exploited to grow large amounts of tissue in which to facilitate repair of extensively damaged nervous systems.

5.2 Stretch-Growth Gene Expression

The central hypothesis is that there are a unique set of genes associated with stretch-growth that are upregulated in response to tension. The objective was to isolate the RNA transcribed from these stretch-grown samples and compare it with RNA from non-stretch-grown controls. Quantification of collected RNA revealed a two-fold increase in stretch-grown tissue. It was further hypothesized that the metabolism of stretch-grown tissue was greatly increased as compared to controls. Future experiments will be

performed in order to determine whether the increased RNA was transported to the axon or remained in the soma.

Though several samples were prepared for DNA microarray analysis, none of the samples were hybridized or processed on the arrays. Due to the time required to optimize the growth and collection of tissue, no microarray experiments could be run within the scope of this report. Microarrays are planned to run shortly following this report as part of a PhD dissertation. Key genes identified by microarray analysis as playing a role in response to varying stretch rate, culture conditions, and treatments will be validated on additional samples with Real Time Polymerase Chain Reactions (Real-Time PCR).

There are broad clinical implications involved in gene expression studies of stretch-grown axons. Discovery of a regulatory pathway could lead to new methods of treatment for debilitating nerve injuries, where current treatments are insufficient to restore nerve function. One such method could be the administration of agonists that provoke the normal stretch-growth response, without the application of tension. Added length in existing nerves may be used to surgically relocate severed nerve endings to their respective targets. Alternatively, such growth may be taken advantage of following stem cell proliferation, through differentiation into neurons, in generation of new nervous tissue.

APPENDIX A

DORSAL ROOT GANGLIA ISOLATION

The following protocol, adapted from Dr. Bryan Pfister, outlines the procedure for isolation of DRGs from pregnant rats.

- Expose E15 pregnant rat with 100% CO₂ for 90 seconds.
- Perform thoracotomy to ensure death.
- Place rat on its back and sterilize the abdomen with 70% ethanol.
- Perform C-section and dissect out the uterus (both sides) and place in sterile dish.

- Under dissection hood, remove embryos from the uterus and place in Leibovitz L-15 medium (Gibco 11415-064) or other non-CO₂ sensitive balanced medium.
- Cut the head off the embryo between the skull and the first vertebra. Using micro scissors or a micro knife, cut on the caudal side of the pronounced bump on the back of the head (between the two pronounced bumps) and under the snout. Leaving some brain stem to handle and pull out the cord.
- With the embryo on its side, remove the anterior portion of the abdomen and limbs with a micro-knife. Place embryo on its back and remove remaining viscera with fine forceps (Dumont #5) until you have a clear view of the vertebral column.
- Beginning at the rostral end, pinch through the vertebral column with fine forceps (Dumont #5).
- Using #4 forceps, grasp the brainstem/ménages and **pull straight up** and place in dish with balanced medium.
- With a fresh pair of #5 Dumont biologine tip forceps, pluck off the DRGs from the isolated spinal cords and place in L-15 medium.

APPENDIX B

DORSAL ROOT GANGLIA PLATING

The following protocol, adapted from Dr. Bryan Pfister, outlines the procedure for plating DRGs.

- Prepare substrates with ECM.
 - PLL poly-L-lysine* (1 hour wet, 1 hour dry).
 - *Note: Live imaging bioreactor is coated with 2% Silane in Acetone for 2 minutes in lieu of PLL.
 - Type-1 Rat-tail Collagen, Becton Dickinson #354236 (polymerize w/ammonia vapor).
- Replace L-15 with culture media and mix cell suspension well.
- Plate DRGs using the drop method (Collagen is hydrophobic and plating is accomplished by placing a drop of cell suspension in desired areas).
 - Bioreactor: for each lane, plate equal aliquots of DRGs on both the towing Aclar and the stationary substrate. The “drop” will be long and slender covering the towing and stationary substrates by 2-3 mm on either side of the interface. Allow cells to incubate at least 2 hours prior to filling with media.
 - Petri dishes: for each dish, plate equal aliquots of DRGs directly into media. Inject cells as evenly as possible to promote spreading.

APPENDIX C

DORSAL ROOT GANGLIA CULTURE

The following protocol, adapted from Dr. Bryan Pfister, outlines the procedure for culture of DRGs.

Cell Maintenance:

- Wednesday: plate cells
- Friday: change media
- Thereafter*: change medium Monday, Wednesday, and Friday.
 - *Note: Stretch-growth experiments do not receive media changes once stretch-growth is initiated.

Media Formulation:

- | | |
|---|-----------|
| • Neuralbasal medium w/ B-27 & 0.4-0.5 mM L-Glut. | 100 mL |
| • 1% FBS heat inactivated CC# 7116 | 98 mL |
| • 20% Glucose Sigma G-7528, 25g in 100mL water | 1 mL |
| • 20 ng/mL (crude) NGF (7S) Gibco 13290-010 | 1 mL |
| • 20 μ M FdU Sigma F-0503 | 2 μ g |
| • 20 μ M Uridine Sigma U-3003 | |

APPENDIX D

STRETCH-GROWTH SPECIFICATIONS

Tables D.1 and D.2 provide specifications for the linear-motion table displacement and stretch-growth schedule.

Table D.1 Step Motor and Table Specifications

	Linear Motion Table
table displacement per rev [μm]	1000
motor steps per rev	5000
μm per step	.2
steps per μm	5

Table D.2 Stretch-growth Schedule

	Time[hr]	[mm/day]	Strain[μm]	Motor Steps	Time between increment[s]	Number of increments	Total length[mm]	Total time[days]
Pretension	24	1	2	10	172.8	500	0	1
Stretch	24	1	2	10	172.8	500	1	2
Stretch	24	2	2	10	86.4	1000	3	3
Stretch	24	3	2	10	57.6	1500	6	4
Stretch	24	4	2	10	43.2	2000	10	5
Stretch	24	5	2	10	34.6	2500	15	6
Stretch	24	6	2	10	28.8	3000	21	7

APPENDIX E

RNA ISOLATION PROTOCOL

The following protocol was used to isolate RNA from control and stretch-grown tissue. The protocol is an adaptation of the Qiagen protocol included with the RNeasy kit used in the experiments.

NOTES:

---Work Quickly, do not attempt more than 2 sample types simultaneously---

---Spinning @ 8000 x g or $\geq 10,000$ RPM---

---Decant after all spinning steps except elution---

---In general, per column:

Lyse between 10^6 and 10^7 cells

Up to 50ug RNA

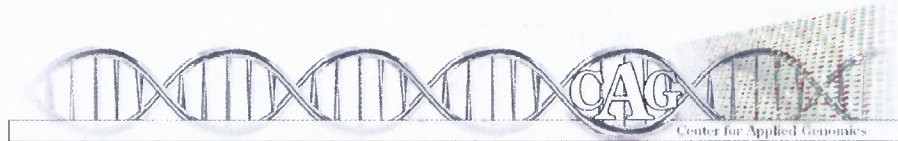
- 1) Aspirate all media & flash freeze on dry ice, (1') 10'
- 2) Using wet ice immerse sample in 1ml buffer RLT w/ 10ul BME
- 3) Homogenize Vortex 1'
- 4) Add 1 volume 70% EtOH
- 5) Transfer samples to columns, 700ul increments
- 6) Spin 15 seconds (keep eluate if uRNA needed)
- 7) DNase Step - Gentle, do not vortex DNase I
 - Add 350ul Buffer RW1, Spin 15 seconds
 - Add 10ul DNase I to 70ul Buffer RDD, mix and spin 80ul, add to column
 - Wait 15' at room temp
 - Add 350ul Buffer RW1, Spin 15 seconds
- 8) Add 500ul Buffer RPE, Spin 15 seconds
- 9) Repeat step #8, Spinning 2'
- 10) Spin full speed w/ new collection tubes 1'
- 11) Using elution tubes, add 30ul RNase-Free H₂O, wait 1', spin 1'
- 12) Take 2→5ul eluate for spec reading & gel, freeze samples -80C

APPENDIX F

RNA GEL ELECTROPHORESIS

The following protocol was used to electrophorese agarose gels and visualize RNA samples for quality. The protocol was provided directly by the Center for Applied Genomics at UMDNJ-New Jersey Medical School.

1. Prepare 1% agarose gel in 1x TBE buffer. Run at 100V, 100mA, 100mA for 1.5 hours. Stain with ethidium bromide and visualize under UV light.



Center for Applied Genomics
 Public Health Research Institute
 UMDNJ - New Jersey Medical School
 www.cag.icph.org

Last update: 2/12/2008

Printed on: 7/15/2008

Protocol for RNA borate gels

Buffers & Solutions

20X RNA Borate Buffer (2L):

400mM Boric Acid	49.46	g
104mM Borax (Sodium Borate)	79.28	g
0.5 M EDTA pH 8.0	16.00	ml

- Prepare on stir plate with low heat to dissolve
- Bring to 2L with ddH₂O in graduated cylinder
- Filter (sterile filter) into sterile bottles

RNA loading dye (non-denaturing):

37% Formaldehyde	165	µl
Formamide	715	µl
20X RNA Borate Buffer	100	µl
10 mg/ml EtBr (under hood in 15 ml conical)	10	µl
2% Bromophenol (in Molecular Grade Water)	10	µl

Store in dark (as light sensitive) and label for safe use.

RNA loading ladder:

0.24-9.5 Kb RNA Ladder,	90	µl
Invitrogen Cat# 15620-016		
RNA loading dye (non-denaturing)	30	µl

- Aliquot in PCR tubes, 8 µl per tube since you need 4µl for the first and last well per gel

Prepare the Gel box

Set up the mold:

- Place the plastic plate on the bottom of the mold. It has to cover the round hole in the bottom of the mold.
- Place the 8 well comb in the mold. To make sure the wells are not too deep, use some tape to elevate the comb.



Make the Gel:

1% agarose-formaldehyde-borate gel (mini):

Agarose	0.5 g
20X RNA Borate Buffer	2.5 ml
ddH ₂ O	43.5 ml

- Microwave for 1'40" and allow to cool until there is no steam anymore
- Add 4ml of 37% formaldehyde, mix and pour gel into the mold
- Let the gel cool down completely

Set up the Gel box:

Dilute 20X RNA Borate Buffer to 1X RNA Borate Buffer before use.

1X RNA Borate Buffer (1L): Running buffer

20X RNA Borate Buffer	50.00 ml
ddH ₂ O	950.00 ml

- Take the solid and cooled gel out of the mold and place it in the gel box.
- Pour the 1X RNA Borate Buffer in the gel box. Make sure the gel is completely submerged.

Prepare the RNA Mix:

RNA Mix

Sample (1µg/µl)	1 µl
ddH ₂ O	2 µl
RNA loading dye	1 µl

- The Sample should contain approximately 1µg of RNA, we assume the concentration of the RNA is 1 µg/µl. If the concentration is lower you may add more Sample to the RNA mix and add less ddH₂O. The final volume of the RNA mix should be 4 µl.

Load and run the Gel

Load the Gel:

- Load 4 µl of RNA Loading Ladder in the first and the last well.
- Load 4 µl of the RNA mix in wells 2 to 7 depending on how many samples you have.

Run the Gel:

- Connect the gel box to the power box.
- Connect the black cable (negative) to the plug that's closest to the wells, RNA runs from negative to positive.
- Connect the red cable to the other plug.
- Set the power box to 100 amp.
- Let it run for 30 minutes.
- Check the gel by putting a white tissue under the gel box. This way you will be able to see if the RNA shifted.
- You may let it run for another 20 minutes.

REFERENCES

1. APACURE Spinal Cord Information
<http://www.apacure.com/>. Retrieved: August 2008
A website with spinal cord and brain injury information.
2. Bray, D. (1984). Axonal Growth in Response to Experimentally Applied Mechanical Tension. *Developmental Biology*, 102, 379-389.
3. Butler S.J., Tear G. (2007). Getting Axons onto the Right Path: the role of transcription factors in axon guidance. *Development*, 134, 439-448.
4. Heidemann S.R., Buxbaum R.E. (1990). Tension as a Regulator and Integrator of Axonal Growth. *Cell Motility and the Cytoskeleton*, 17, 6-10.
5. Huang J.H., Zager E.L., Zhang J., Groff R.F., Pfister B.J., Cohen A. S., Grady M.S., Wilensky E. M., Smith D.H. (2008). Harvested Human Neurons Engineered as Live Nervous Tissue Constructs: implications for transplantation. *Journal of Neurosurgery*, 108, 343-347.
6. Iwata A., Browne K.D., Pfister B.J., Gruner J.A., Smith D.H. (2006). Long-Term Survival and Outgrowth of Mechanically Engineered Nervous Tissue Constructs Implanted into Spinal Cord Lesions. *Tissue Engineering*, 12, 101-110.
7. Kindler S., Wang H., Richter D., Tiedge H. (2005). RNA Transport and Local Control of Translation. *Annual Review of Cell and Developmental Biology*, 21, 223-245.
8. Lin A.C., Holt C.E. (2007). Local Translation and Directional Steering in Axons. *EMBO Journal*, 26, 3729-3736.
9. Miller, K.E., Sheetz M.P. (2006) Direct evidence for Coherent Low Velocity Axonal Transport of Mitochondria. *Journal of Cell Biology*, 173, 373-381.
10. Pfister B.J., Bonislowski D.P., Smith D.H., Cohen A.S. (2006). Stretch-Grown Axons Retain the Ability to Transmit Active Electrical Signals. *FEBS Letters*, 508, 3525-3531.
11. Pfister B.J., Huang J.H., Zager E.L., Smith D.H. (2007). Neural Engineering To Produce In Vitro Nerve Constructs and Neurointerface. *Neurosurgery*, 60, 137-142.

12. Pfister B.J., Iwata A., Meaney D.F., Smith D.H. (2004). Extreme Stretch Growth of Integrated Axons. *Journal of Neuroscience*, 24, 7978-7983.
13. Pfister B.J., Iwata A., Taylor A.G., Wolf J.A., Meaney D.F., Smith D.H. (2006). Development of Transplantable Nervous Tissue Constructs Comprised of Stretch-Grown Axons. *Journal of Neuroscience Methods*, 153, 95-103.
14. Quackenbush J. (2001). Computational Analysis of Microarray Data. *Nature*, 2, 418-427.
15. Spinal Cord Injury Information Network
<http://www.spinalcord.uab.edu/>. Retrieved: August 2008
A website with information and statistics about SCI.
16. Tyagi S., Kramer F.R. (1995). Molecular Beacons: probes that fluoresce upon hybridization. *Nature Biotechnology*, 14, 303-308.
17. Vargas D.Y., Raj A., Marras S.A.E., Kramer F.R., Tyagi S. (2005). Mechanism of mRNA Transport in the Nucleus. *PNAS*, 102, 17008-17013.
18. Weiss P. (1941). Nerve patterns: The Mechanics of Nerve Growth. *Growth, Third Growth Symposium*, 5, 163-203.
19. Willis D., Li K.W., Zheng J.Q., Chang J.H., Smit A., Kelly T., Merianda T.T., Sylvester J., Minnen J.V., Twiss J.L. (2005). Differential Transport and Local Translation of Cytoskeletal, Injury-Response, and Neurodegeneration Protein mRNAs in Axons. *Journal of Neuroscience*, 25, 778-791.